U

SECURITY CLASSIFICATION OF THIS PAGE

REPORT DOCUMENTATION PAGE

Form Approved OMB No 0704-0188

1a REPORT SECURITY CLASSIFICATION: (U)	1b RESTRICTIVE MARKINGS: NA
2a SECURITY CLASSIFICATION AUTHORITY: NA	3 DISTRIBUTION/AVAILABILITY OF REPORT: Unlimited
2b DECLASSIFICATION/DOWNGRADING SCHEDULE: NA	
4 PERFORMING ORGANIZATION REPORT NUMBER(S)	5 MONITORING ORGANIZATION REPORT NUMBER(S): NA
6a NAME OF PERFORMING ORGANIZATION: University of Illinois at Urbana-Champaign	6b OFFICE SYMBOL (If applicable): NA
7a NAME OF MONITORING ORGANIZATION: Office of Naval Research	
6c ADDRESS (City, State, and ZIP Code): 1110 West Green Street, Urbana, IL 61801	7b ADDRESS (City, State, and ZIP Code): 800 North Quincy Street, Arlington, VA 22217-5000
8a NAME OF FUNDING/SPONSORING ORGANIZATION: Office of Naval Research	8b OFFICE SYMBOL (If applicable): ONR
9 PROCUREMENT INSTRUMENT IDENTIFICATION NUMBER: N00014-89-J-1300	
8c ADDRESS (City, State, and ZIP Code): 800 North Quincy Street, Arlington, VA 22217-5000	10 SOURCE OF FUNDING NUMBERS

PROGRAM ELEMENT NO	PROJECT NO	TASK NO	WORK UNIT ACCESSION NO
61153N	RR04106	4413015-05	

11 TITLE (Include Security Classification)

(U) Pressure Studies of Protein Dynamics

12 PERSONAL AUTHOR(S)

Hans Frauenfelder and Robert D. Young

13a TYPE OF REPORT	13b TIME COVERED	14 DATE OF REPORT (Year, Month, Day)	15 PAGE COUNT
Annual	FROM 3/89 TO 2/90	90/2/28	

16 SUPPLEMENTARY NOTATION

17 COSATI CODES			18 SUBJECT TERMS (Continue on reverse if necessary and identify by block number)
FIELD	GROUP	SUB-GROUP	Pressure, protein dynamics, myoglobin, heme proteins, conformational substates, Photolysis, Resonance Spectroscopy

19 ABSTRACT (Continue on reverse if necessary and identify by block number)

Our work during the past decade has shown conclusively that the energy landscape of proteins is complex: The ground state of proteins is highly degenerate and consists of a very large number of energy valleys separated by energy mountains and ridges. Moreover, the energy landscape may be hierarchical and contain valleys within valleys. Evidence is mounting that many, maybe all, complex systems are characterized by a highly degenerate and hierarchicaly arranged ground state. Among such systems and problems are glasses, spin glasses, evolution, learning, neural networks, computer and chip design, and the traveling salesman problem. Proteins consequently may be models for many other systems and progress in protein dynamics may have impact on these other fields.

We investigate three aspects of protein dynamics: (1) the structure and organization of the energy landscape, (2) conformational motions (dynamics), and (3) the laws governing the motions (reaction theory). In all three aspects, we intend to study the phenomena in one protein (myoglobin) in detail and then explore how the phenomena depend on changes in protein structure.

20 DISTRIBUTION/AVAILABILITY OF ABSTRACT	21 ABSTRACT SECURITY CLASSIFICATION
☒ UNCLASSIFIED/UNLIMITED ☐ SAME AS RPT ☐ DTIC USERS	(U)

22a NAME OF RESPONSIBLE INDIVIDUAL	22b TELEPHONE (Include Area Code)	22c OFFICE SYMBOL
M. Marron	202/696-4760	ONR

DD Form 1473, JUN 86 — Previous editions are obsolete — SECURITY CLASSIFICATION OF THIS PAGE

S/N 0102-LF-014-6603

Our experimental approach combines two main techniques (flash photolysis and Fourier-Transform Infrared Spectroscopy), applied over wide ranges in temperature (10-330K), time (ps-ks), pressure (0.1-200 MPa), solvent conditions and pH to a wide variety of heme proteins. We monitor protein reactions and relaxations from the near ultraviolet to the mid-infrared. Access to proteins specifically designed by genetic engineering permits us to ask very focused questions concerning the role of crucial amino acids in protein function and dynamics. Central in our work is the use of pressure, both as static parameter and as perturbation to study protein relaxation. To our knowledge we are the only group in protein research to systematically use temperature and pressure over wide ranges.

PRESSURE STUDIES OF PROTEIN DYNAMICS

Hans Frauenfelder and Robert D. Young
Principal Investigators

Department of Physics
University of Illinois at Urbana-Champaign

Annual Report - Year 1

ONR Contract N00014-89-J-1300 R&T Code 4413015-05
Starting Date: 1 March 1989

1. INTRODUCTION

Work in our laboratory and others shows that the energy landscape of a protein is complex consisting of a large number of energy valleys separated by energy mountains and ridges. Moreover, experimental and theoretical evidence is accumulating that the energy landscape is hierarchical and contains valleys within valleys. We continue our investigation of several aspects of protein dynamics; (i) the structure and organization of the energy landscape focusing on the hierarchical nature of the landscape, (ii) protein motions within the energy landscape, (iii) the laws governing the motions, and (iv) the slaved glass transition in proteins. We also attempt to uncover the laws of protein reactions under pressure (reaction theory).

We study phenomena in detail in one protein (myoglobin) and then explore how the phenomena depend on protein structure. To do this we move to other, possibly more complicated, proteins and to synthetic mutant myoglobins. Our experimental approach involves flash photolysis applied over wide ranges in temperatures (10 to 330K), time (ns to ks), and pressure (0.1 to 300 MPa). Pressure is central to our work both as static parameter and dynamic perturbation to probe protein relaxations. We monitor protein reactions and relaxations from the near ultraviolet to the mid-infrared with Fourier

Transform Infrared Spectroscopy playing an essential role. We also use theoretical and computational tools to build models of protein dynamics and reactions.

2. ACCOMPLISHMENTS

Progress has been very good during the first year. A short paper entitled "Glassy Behavior of a Protein" has been published which shows that proteins and glasses share essential characteristics (1). In particular we proved that myoglobin, like glasses, exhibits metastability below a transition temperature and relaxation processes that are nonexponential in time and non-Arrhenius in temperature. A second, much longer, manuscript entitled "Proteins and Pressure" has appeared in the Journal of Physical Chemistry (2). This manuscript describes many of our discoveries regarding protein relaxations and reactions obtained using wide ranges of pressure and temperature. These results greatly clarify the effects of pressure and imply that most previous work on pressure effects in proteins needs to be reexamined. Both papers are included in the Appendix to this Report. Our work also includes the following activities:

(i) Pressure Effects on CO Binding to Myoglobin. We performed a series of experiments using FTIR spectroscopy to probe the effects of pressure on the kinetics of CO binding to the different A substates of myoglobin after photodissociation below 100K. The A substates involve tier 0 of the hierarchy of substates. We use different pathways in the pressure-temperature plane to separate conformational (equilibrium) and kinetic phenomena. These experiments clearly demonstrate the subtle and important effects of pressure on protein dynamics and function. Our main results appear in the paper "Proteins and Pressure" (2).

(ii) Pressure-Temperature Studies of Horse and Sperm Whale Myoglobin. The kinetics of horse and sperm whale myoglobin are very similar at atmospheric pressure even when temperature is varied over a wide range. However studies on these two mammalian myoglobins over wide ranges of temperature and pressure reveal significant differences

which are mainly a result of conformational effects (2). It is interesting to speculate if these differences are related to the fact that whales must dive but horses do not!

(iii) Quasistatic and Kinetic Studies of More Complicated Heme Proteins. We have begun to study the effects of protein structure using the more complicated heme proteins horseradish peroxidase type C (HRP-C) and cytochrome P450. We use CO binding to the heme iron in HRP-C and P450 to probe the slaved glass transition and protein relaxation processes. Using pressure, we have observed CO stretch bands in HRP-C-CO which correspond to protein structures not previously resolved. P450 with substrate bound and unbound has also yielded surprising results. We have begun to study the complex spectrum of relaxation processes in these proteins near the slaved glass transition and have presented preliminary reports of our results at the March Meeting of the American Physical Society (3) and the Meeting of the Biophysical Society (4). We will continue our studies concentrating on samples and conditions of temperature and pH where the pressure effects are particularly dramatic. This work may give significant new information regarding the substates of tier 0 (CS^0) which we believe are crucial to protein function.

(iv) General Aspects – Pressure and Proteins. Our previous work has shown that the substates of tier 0 in myoglobin (A substates) have different kinetics for rebinding CO and are affected differently by pressure. The manuscript "Proteins and Pressure" (2) also includes a reexamination of our previous work, much of it unpublished, on pressure effects in proteins. We analyze in detail the subtle but crucial effects of the different protein structures corresponding to tier 0 (CS^0) of the hierarchy of substates in myoglobin. Since the different substates of CS^0 also bind CO at different rates and have different structures and volumes, the switch from one substate to another provides the possibility of an efficient control mechanism. We have shown in Ref. (2) that the effects of pressure in the visible spectral region can be very misleading since this spectral region is not sufficiently sensitive to conformational effects.

3. CONCLUSIONS

The technique and results under this contract may be important for both biology and physics. For biology, detailed knowledge of protein motions at different time and length scales is necessary for an understanding of protein and enzyme reactions at the molecular level. In particular the different behavior between horse and whale myoglobin under pressure is intriguing and calls for further studies. For physics, proteins may well become paradigms of complex systems including glasses, spin glasses, and neural networks. References (1) and (2) can be consulted for additional details and discussion.

4. REFERENCES AND PUBLICATIONS

(Year 1 – March 1989 to February 1990. Supported in part by this contract.)

References indicated by asterisk * are included as part of this report.

* 1. Iben, I. E. T., Braunstein, D., Doster, W., Frauenfelder, H., Hong, M. K., Johnson, J. B., Luck, S., Ormos, P., Schulte, A., Steinbach, P. J., Xie, A. H. & Young, R. D. Glassy Behavior of a Protein. Phys. Rev. Lett. **62**, 1916-1919 (1989).

* 2. Frauenfelder, H., Alberding, N. A., Ansari, A., Braunstein, D., Cowen, B. R., Hong, M. K., Iben, I. E. T., Johnson, J. B., Luck, S., Marden, M. C., Mourant, J. R., Steinbach, P. J., Xie, A., Young, R. D. & Yue, K. T. Proteins and Pressure. J. Phys. Chem. **94**, 1024-1037 (1990).

3. Scholl, R., Braunstein, D., Frauenfelder, H., Hager, L. P., Hong, M. K., Johnson, J. B., Suh, Y. J., Xie, A. H. & Young, R. D. Pressure-Temperature Studies on Carbonmonoxy Horseradish Peroxidase (HRP-CO). Bull. Am. Phys. Soc. **34**, 417 (1989). Abstract.

4. Scholl, R., Blanke, S. R., Chu, K., Ehrenstein, D., Frauenfelder, H., Hager, L. P., Johnson, J. B., Jung, C., Mourant, J. R., Philipp, R., Sligar, S. G., Stayton, P., Suh, Y. J. & Young, R. D. Relaxation Dynamics in Carbonmonoxy Hemeproteins. Biophys. J. **57**, 233a (1990). Abstract.

5. Frauenfelder, H., Steinbach, P. J. & Young, R. D. Conformational Relaxation in Proteins. Chemica Scripta **29A**, 145-150 (1989).

6. Frauenfelder, H. The Debye-Waller Factor: From Villain to Hero in Protein Crystallography. Int. J. Quan. Chem. **35**, 711-715 (1989).

7. Young, R. D. Glassy Dynamics in Proteins. In *Cooperative Dynamics in Complex Physical Systems*, Ed. H. Takayama (New York:Springer, 1989) p. 203.

8. Ormos, P., Ansari, A., Braunstein, D., Cowen, B. R., Frauenfelder, H., Hong, M. K., Iben, I. E. T., Sauke, T. B., Steinbach, P. J. & Young, R. D. Inhomogeneous Broadening in Spectral Bands of Carbonmonoxymyoglobin. Biophys. J. **57**, 191-199 (1990).

Glassy Behavior of a Protein

I. E. T. Iben,[1],[a] D. Braunstein,[1] W. Doster,[2] H. Frauenfelder,[1] M. K. Hong,[1] J. B. Johnson,[1] S. Luck,[1] P. Ormos,[1],[b] A. Schulte,[1],[c] P. J. Steinbach,[1] A. H. Xie,[1] and R. D. Young[1],[3]

[1]*Department of Physics, University of Illinois, 1110 West Green Street, Urbana, Illinois 61801*

[2]*Physik Department, Technische Universität München, D-8046 Graching, Federal Republic of Germany*

[3]*Department of Physics, Illinois State University, Normal, Illinois 61761*

(Received 16 June 1988)

Quasistatic and kinetic studies of the infrared CO stretch bands of carbonmonoxymyoglobin show that proteins and glasses share essential characteristics, in particular metastability below a transition temperature and relaxation processes that are nonexponential in time and non-Arrhenius in temperature.

PACS numbers: 87.15.Da, 64.70.Pf, 78.30.Jw, 82.20.Rp

Proteins and glasses may appear to have little in common. Proteins are macromolecules with well defined structures[1]; glasses are frozen liquids. Despite this difference, proteins and glasses share one fundamental property: Both can assume a very large number of nearly isoenergetic conformational substates (CS), valleys in the conformational energy landscape. For proteins, the existence of CS followed from the nonexponential time dependence of the binding of small molecules (O_2 and CO) to myoglobin at low temperatures.[2] Supporting evidence came from other experiments[3] and from theory.[4] For glasses, a potential-energy surface with a large number of minima was postulated by Goldstein[5]; for spin glasses, the evidence came from theory.[6] The existence of CS in proteins and glasses raises the question as to whether these systems share other properties. We now describe some attributes of glasses and later show that these are also found in proteins.[7]

Glasses are formed when, on cooling, a liquid becomes a structurally disordered solid.[8] The temperature at which the viscosity reaches 10^{13} poise is called the glass temperature, T_g. The specific heat below 1 K is approximately proportional to the temperature.[9] Glass properties well below T_g depend on history; glasses are in a metastable (nonequilibrium) state. Near and above T_g the response of a glass to a mechanical or electrical perturbation is dominated by the α relaxation. Its relaxation function $\Phi_r(t)$ is usually nonexponential in time and can be parametrized by a stretched exponential, $\Phi_r(t) = \exp[-(kt)^\beta]$, or by a power law,

$$\Phi_r(t) = [1 + k_r(T)t]^{-n}. \quad (1)$$

The average rate at temperature T is $\langle k \rangle = nk_r(T)$. The temperature dependence of $k_r(T)$ follows the Arrhenius relation, $k_r(T) = A\exp[-E/k_BT]$, only over small temperature intervals. Typical values near T_g, $E \approx 1.6$ eV, $A = 10^{42}$ s^{-1}, also imply that the Arrhenius relation is inappropriate for glasses. However, $k_r(T)$ can be described over more than 10 orders of magnitude either by the Vogel-Tammann-Fulcher equation,[8]

$$k_r(T) = A_{VTF}\exp[-E/k_B(T - T_0)] \quad (2)$$

or by the relation[10,11]

$$k_r(T) = k_0\exp[-(T_0/T)^2]. \quad (3)$$

Both relations fit the data for glycerol ($T_g \approx 185$ K) from 190 to 260 K.[10,12]

We now examine the proteins for glasslike properties. Two are well known: Each individual protein is disordered (aperiodic) and the specific heat of proteins below 1 K is glasslike.[13] The other attributes, however, have been less well explored. Here we report experiments that verify the metastability at low temperatures, and the nonexponential time and the non-Arrhenius temperature dependence of the protein relaxations near 200 K in carbonmonoxymyoglobin (MbCO).

The folded polypeptide chain of the oxygen-storage protein myoglobin (Mb) embeds a heme group with a central iron atom which reversibly binds ligands such as O_2 and CO.[1] Our experiments focus on the stretch bands of CO bound to Mb which are very sensitive to external parameters such as solvent, *p*H, temperature (T), and pressure (P).[14,15] We measure the stretch bands with a Mattson Fourier transform infrared spectrometer. Figure 1 shows that MbCO displays at least three different CO stretch bands, A_0, A_1, and A_3. Fits to Voigtian line shapes[16] yield the areas (A_i), center frequencies (ν_i), and linewidths (Γ_i) of the A bands. We also observe the rate of heat absorption via differential scanning calorimetry (DSC). The experiments fall into two classes, quasistatic and kinetic. Quasistatic indicates that the glasslike behavior of MbCO below a transition temperature T_{sg} prevents attainment of thermodynamic equilibrium. Quasistatic measurements determine the band parameters as functions of solvent, *p*H, T, and P. In the kinetic studies we observe the relaxation of the protein after a pressure release.

Quasistatic experiments.—Figure 1 shows the ir spectra from 1910 to 1990 cm^{-1} in a 75% glycerol-water solvent (3:1 by volume) at *p*H 6.8 with potassium phosphate buffer. The sample was brought to a pressure P at 300 K. Data were then taken under constant pressure at successively lower temperatures. The cooling rate of 0.01 K/s and waiting time of about 600 s at each temper-

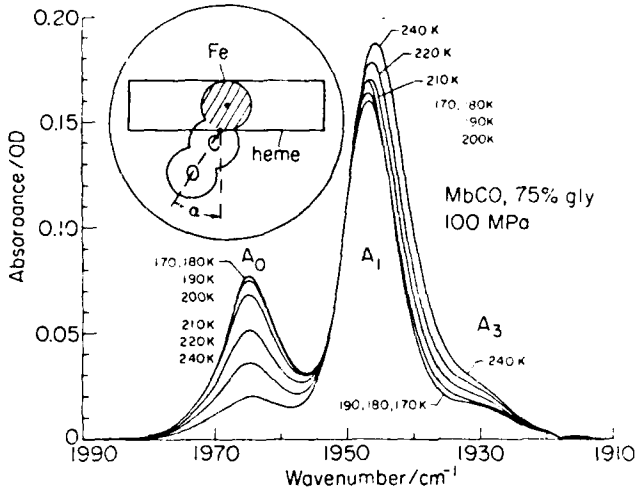

FIG. 1. Absorption spectra of the CO stretch bands of MbCO at 100 MPa. Solvent: 75% glycerol and water mixture, buffered with 100 mM potassium phosphate to pH 6.8. Inset: Cross section through the heme showing the angle α, between the CO dipole and the heme normal.

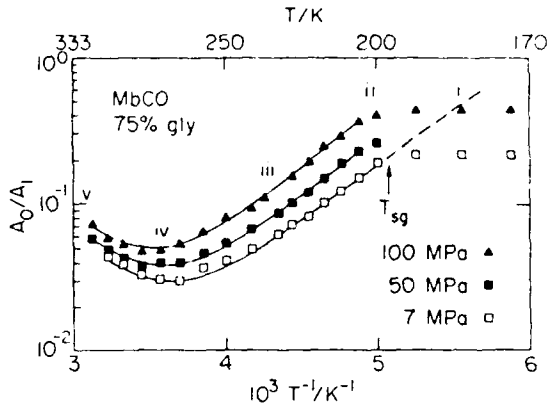

FIG. 2. Plot of $r_0 = A_0/A_1$ vs $10^3/T$ for three pressures. Roman numerals signify the five temperature regions defined in the text. The transition temperature T_{sg} is indicated. The dashed line shows the extrapolation from region (iii) for 7 MPa.

ature were kept constant. Measurement of an ir spectrum took about 250 s. Figure 2 gives the temperature dependence of the ratio $r_0 = A_0/A_1$ at three different pressures. The ratio r_0 exhibits five regions: (i) *Glass region.* The protein is in a metastable state in which large-scale motions are too slow to be observed. We prove metastability by showing that the ir spectrum depends strongly on the path by which a point in the (T,P) plane is reached. (ii) *Slaved glass transition.* The bend at T_{sg} in Fig. 2 reveals the transition from an equilibrium situation well above T_{sg} to a metastable one well below. A similar bend occurs in $\Gamma(T)$,[14] and the transition is also visible in DSC. The glass temperature T_{sg} of the protein depends crucially on the glass temperature T_g of the solvent; so we call the transition "slaved"[14]: DSC data at a heating rate of 0.083 K/s in 75% glycerol and water mixture give $T_g = 175$ K and $T_{sg} = 178$ K; in 60% ethylene-glycol-water mixture $T_g = 149$ K and $T_{sg} = 155$ K; in solid poly(vinyl)alcohol $T_g > 280$ K and $T_{sg} > 280$ K. T_{sg} and T_g depend approximately logarithmically on cooling or heating rate; a factor of 10 increase in heating rate raises T_{sg} by about 5 K. T_{sg} obtained from the bend in r_0 is about 20 K higher than that from DSC. With increasing pressure T_{sg} increases weakly as is apparent from Fig. 2. (iii) *Lower equilibrium region.* Transitions among the A substates occur faster than the time of observation so that the A substates are in thermal equilibrium. The temperature and pressure dependences of the ratios r_i determine the relative energies, entropies, and volumes of the A substates. (iv) *Upper equilibrium region.* From 250–320 K, the ratio r_0 shows a remarkable reversal. (v) *Unfolding.*[17] The protein begins to unfold irreversibly. Since regions (iv) and (v) are not the focus of this Letter we give no further details.

Relaxation experiments.— In a pressure-release experiment, 100 MPa is applied at 240 K, the sample is cooled to the desired temperature and held there for 600 s followed by measurement of an ir spectrum for about 250 s. The pressure is then released to 7 MPa in a few seconds and ir spectra are taken at approximately exponentially increasing times from about 10 to more than 10^4 s. The time-dependent behavior of the A bands after pressure release reveals several relaxation processes. To interpret the relaxation data, we assume that the conformational substates of a protein are arranged in a hierarchy of at least two tiers, CS^0 and CS^1.[14,18] The different stretch bands correspond to substates of tier 0 (CS^0). We characterize each substate A_i by the center frequency ν_i of the CO stretch band (Fig. 1) and by the angle α_i between the CO dipole and the heme normal (inset of Fig. 1).[19] It is likely that the substates A_i differ not only in the angle α_i, but also in the overall structure of the molecule. A protein may move from one substate of tier 0, say A_0, to another, say A_1. We call this motion FIM 0, where FIM is an acronym for "functionally important motion."[18] Rebinding of CO after flash photolysis to each of the A substates is nonexponential in time.[14] This observation implies that each substate of tier 0 is subdivided into substates of tier 1, CS^1. We denote as FIM 1 the nonequilibrium conformational motions between substates of tier 1. With these concepts we explain our experiments.

Below 160 K.— The center frequencies of the A bands shift (0.4 cm^{-1} for A_0) faster than our shortest measurement time (10 s), but no changes in relative intensities occur up to 10^4 s. Since the fast shift occurs even at 15 K, we interpret it as an elastic relaxation.

165–185 K.— The area of A_0 remains constant to within 2% from 10 to more than 10^4 s while the peak narrows and its amplitude increases. The center fre-

quency ν_0 ir ..y shifts rapidly from 1964.5 to 1964.9 cm^{-1} and then moves measurably towards its low-pressure value, 1966.1 cm^{-1}. The shift in ν_0 can be described by a relaxation function $\Phi_1(t) = [\nu_0(t) - \nu_t(\infty)]/[\nu_0(0^+) - \nu_0(\infty)]$, where t is the time after pressure release and $\nu_0(0^+)$ represents the center frequency immediately after the rapid elastic relaxation. For $\nu_0(\infty)$ we use two approximations, the 7 MPa value from a quasistatic experiment at the same temperature and the value obtained by extrapolation from region (iii). Figure 3 shows the relaxation function $\Phi_1(t)$ using the former choice for $\nu_0(\infty)$. $\Phi_1(t)$ is not greatly changed with the other choice. We interpret the relaxation characterized by Φ_1 as FIM 1, a redistribution of substates CS^1 within the substate A_0.

To evaluate the data in Fig. 3, we parametrize $\Phi_1(t)$ by the power-law equation (1).[20] If we further assume that $k_r(T)$ is determined by the Arrhenius law, we obtain $E = 1.3$ eV, $A = 10^{36}$ s^{-1}. These values are similar to the values quoted above for the α relaxation in glasses near T_g; they imply that the Arrhenius relation is inappropriate for describing FIM 1 and suggest the use of Eq. (2) or (3). We select Eq. (3) to fit $k_r(T)$ because it uses only two parameters and therefore provides less ambiguous extrapolations. A fit with Eqs. (1) and (3), using a Levenberg-Marquardt algorithm to minimize χ^2, is shown as solid lines in Fig. 3 and yields $\log(k_0/s^{-1}) = 17.0 \pm 2.5$, $T_0 = 1130 \pm 80$ K, $n = 0.26 \pm 0.12$. The errors are conservative. We have also measured the α relaxation in 75% glycerol and water mixture using specific-heat spectroscopy[12] and obtain $\log(k_0/s^{-1}) \approx 18$ and $T_0 \approx 1130$ K. The values of k_0 and T_0 for the protein and the solvent are remarkably close and support the notion of a slaved-glass transition: Not only do the solvent and protein exhibit comparable glass temperatures, the α relaxation of the solvent and FIM 1 in the protein obey nearly identical temperature dependences.

A second relaxation, not shown here, occurs between 170 and 190 K: A_1 and A_3 interconvert, with A_1 decreasing and A_3 increasing nonexponentially in time; the barrier between A_1 and A_3 is smaller than that between A_0 and the other A substates.[21]

190–210 K.—FIM 1 and the interconversion between A_1 and A_3 are faster than 10 s so that after pressure release the center frequencies, the linewidths, and the ratio A_3/A_1 have the values measured quasistatically at 7 MPa. A new relaxation process is observed, the exchange of A_0 with $A_1 + A_3$. We interpret this exchange among substates of tier 0 as a conformational change of the entire protein and call it FIM 0. We define a relaxation function for FIM 0 through $\Phi_0(t) = [A_0(t) - A_0(\infty)]/[A_0(0^+) - A_0(\infty)]$. The area $A_0(\infty)$ is found by extrapolation from region (iii) as indicated by the dashed line in Fig. 2.[21] $\Phi_0(t)$, shown in Fig. 4, displays more structure than FIM 1 and a simple power law or stretched exponential does not fit the data well. Nevertheless, insight is gained by fitting the data with Eqs. (1) and (3), with the result $\log(k_0/s^{-1}) \approx 14$, $T_0 \approx 1200$ K, $n \approx 0.8$. The fit reproduces the general behavior of $\Phi_0(t)$, but the detailed structure will require a more elaborate model.

Our results permit four conclusions: (1) Proteins and glasses indeed share common properties in addition to the existence of many valleys (conformational substates) in the energy landscape. The similarities include metastability below the glass temperature and the presence of a relaxation process governing large-scale motions (α relaxation in glasses, FIM 1 in proteins) which is nonexponential in time and does not follow the Arrhenius law. (2) While glasses usually show only one relaxation process with the general characteristics of the α relaxation, MbCO shows at least two, FIM 0 and FIM 1. FIM 0 is slower than FIM 1 and probably describes overall changes in the entire protein, characterized by different CO stretch frequencies and angles between the bound CO and the heme normal. FIM 1 describes large-scale motions within a given substate CS^0. (3) The protein relaxation process FIM 1 is slaved to the solvent; the transition temperature T_{sg} in the protein is close to the glass transition of the solvent. Moreover, FIM 1 in the protein

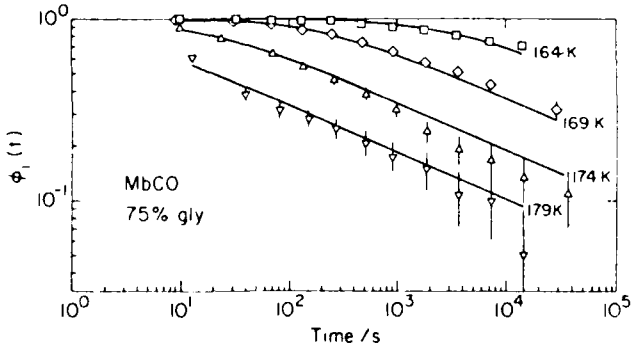

FIG. 3. Relaxation function $\Phi_1(t)$ for the center frequency ν_0 of the A_0 band vs time. Solid lines are fits with Eqs. (1) and (3) with parameters as given in the text.

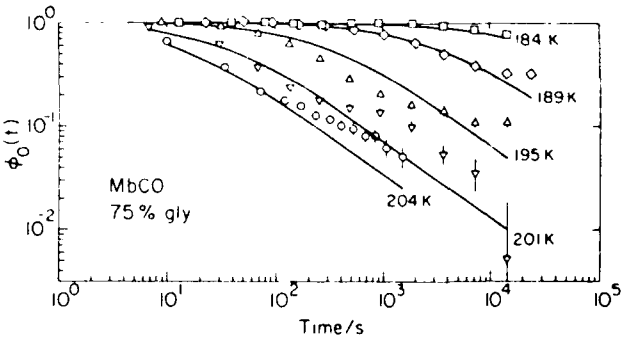

FIG. 4. Relaxation function $\Phi_0(t)$ for the area A_0 vs time. Solid lines are fits with Eqs. (1) and (3) with parameters as given in the text.

and the α relaxation in the solvent, at least in the case of glycerol and water, possess remarkably similar temperature and time dependences. The hydration shell may well play an important role in this coupling between protein and solvent.[22] (4) FIM 0 and FIM 1 can be extrapolated to 300 K with Eq. (3) with the result $\langle k \rangle \approx 10^7$ s^{-1} for FIM 0 and $\langle k \rangle \approx 10^{10}$ s^{-1} for FIM 1. While these extrapolations are speculative, they indicate where to look experimentally and suggest that molecular dynamics[23] may be able to simulate FIM 1 but probably cannot yet reach FIM 0.

The technique and the results presented here may be important for both physics and biology. For physics, proteins may well become paradigms of complex systems. The combination of the pressure jump approach with site-specific spectroscopic observation permits site-specific studies of relaxation phenomena in amorphous systems. When applied to genetically engineered proteins,[24] the pressure jump technique would probe the relaxation of specifically designed systems. For biology, detailed knowledge of protein motions at different time and length scales is necessary for an understanding of protein and enzyme reactions at the molecular level. Slaving may be an efficient control mechanism in cells and membranes.

We thank Professor Harry Drickamer, Professor Ray Orbach, and Professor Peter Wolynes for discussions and advice. We also thank Joel Berendzen, Ben Cowen, and Reinhard Scholl for helpful comments. H.F. acknowledges financial assistance from the Humboldt Foundation. R.D.Y. acknowledges support from NSF Grant No. INT 87-00274 and the Hungarian Academy of Sciences. This work was partially supported by U.S. National Institutes of Health Grants No. GM 18051 and No. GM 32455, National Science Foundation Grants No. DMB 82-09616 and No. DMB 88-16476, and Office of Naval Research Grant No. N00014-86-K-0270.

[a]Current address: AT&T Bell Laboratories, 1A-135, 600 Mountain Avenue, Murray Hill, NJ 07974.

[b]Current address: Institute of Biophysics, Hungarian Academy of Sciences, Odesszai Krt. 62, 6701 Szeged, Hungary.

[c]Current address: IBM, Almaden Research Laboratories, Almaden Valley, CA 95120.

[1]L. Stryer, *Biochemistry* (Freeman, San Francisco, CA, 1988).

[2]R. H. Austin *et al.*, Phys. Rev. Lett. **32**, 403 (1974), Biochemistry **14**, 5355 (1975).

[3]H. Frauenfelder, F. Parak, and R. D. Young, Annu. Rev. Biophys. Biophys. Chem. **17**, 451 (1988).

[4]D. Stein, Proc. Natl. Acad. Sci. U.S.A. **82**, 3670 (1985); R. Elber and M. Karplus, Science **235**, 318 (1987); N. Gō and T. Noguti, Chem. Scr. (to be published).

[5]M. Goldstein, J. Chem. Phys. **51**, 3728 (1969).

[6]P. W. Anderson, Phys. Today **41**, No. 9, 9 (1988); R. G. Palmer, Adv. Phys. **31**, 669 (1982), M. Mézard *et al.*, Phys. Rev. Lett. **52**, 1156 (1984); K. Binder and A. P. Young, Rev. Mod. Phys. **58**, 801 (1986).

[7]We compare a single protein molecule (not a protein ensemble) to a glass sample. At sufficiently low temperatures, a protein molecule or a glass sample occupies a single CS. With increasing temperature, a glass liquifies and a protein moves from CS to CS. Refreezing captures a protein or a glass again in a single CS.

[8]R. Zallen, *The Physics of Amorphous Solids* (Wiley, New York, 1983); J. Jäckle, Rep. Prog. Phys. **49**, 171 (1986); S. Brawer, *Relaxation in Viscous Liquids and Glasses* (American Ceramic Society, Columbus, OH, 1985); in *Molecular Dynamics and Relaxation Phenomena in Glasses*, edited by T. Dorfmüller and G. Williams, Lecture Notes in Physics, Vol. 277 (Springer-Verlag, Berlin, 1987).

[9]W. A. Phillips, Rep. Prog. Phys. **50**, 1657 (1987).

[10]H. Bässler, Phys. Rev. Lett. **58**, 767 (1987); M. Grunewald *et al.*, Philos. Mag. B **49**, 341 (1984).

[11]R. Zwanzig, Proc. Natl. Acad. Sci. U.S.A. **85**, 2029 (1988).

[12]Y. H. Jeong, S. R. Nagel, and S. Bhattacharya, Phys. Rev. A **34**, 602 (1986); N. O. Birge and S. R. Nagel, Phys. Rev. Lett. **54**, 2674 (1985), P. Kuhns and M. S. Conradi, J. Chem. Phys. **77**, 1771 (1982); Å. Fransson and G. Bäckstrom, Int. J. Thermophys. **8**, 851 (1987).

[13]V. I. Goldanskii, Yu. F. Krupyanskii, and V. N. Fleurov, Dok. Akad. Nauk SSSR **272**, 978 (1983), G. P. Singh *et al.*, Z. Phys. B **55**, 23 (1984).

[14]A. Ansari *et al.*, Biophys. Chem. **26**, 337 (1987).

[15]M. W. Makinen, R. A. Houtchens, and W. S. Caughey, Proc. Natl. Acad. Sci. U.S.A. **76**, 6042 (1979); E. G. Hamingo and J. O. Alben, Biochemistry **24**, 7964 (1985).

[16]C. J. Batty, S. D. Heath, and B. L. Roberts, Nucl. Instrum. Methods **137**, 179 (1976).

[17]R. Jaenicke, Prog. Biophys. Mol. Biol. **49**, 117 (1987).

[18]A. Ansari *et al.*, Proc. Natl. Acad. Sci. U.S.A. **82**, 5000 (1985).

[19]J. Kuriyan *et al.*, J. Mol. Biol. **192**, 133 (1986), P. Ormos *et al.*, Proc. Natl. Acad. Sci. U.S.A. **85**, 8492 (1988).

[20]The power law provides better fits to our data than does the stretched exponential.

[21]I. E. T. Iben, Ph.D. dissertation, University of Illinois at Urbana-Champaign, 1988 (unpublished).

[22]G. Careri, P. Fasella, and E. Gratton, Ann. Rev. Biophys. Bioeng. **8**, 69 (1979); G. P. Singh *et al.*, Phys. Rev. Lett. **47**, 685 (1981); W. Doster *et al.*, Biophys. J. **50**, 213 (1986).

[23]J. A. McCammon and S. C. Harvey, *Dynamics of Proteins and Nucleic Acids* (Cambridge U. Iv. Press, New York, 1987); C. L. Brooks, M. Karplus, and B. M. Pettitt, *Proteins: A Theoretical Perspective of Dynamics, Structure and Thermodynamics* (Wiley, New York, 1988).

[24]D. Braunstein *et al.*, Proc. Natl. Acad. Sci. U.S.A. **85**, 8497 (1988).

Proteins and Pressure

Hans Frauenfelder,* Neil A. Alberding,† Anjum Ansari,‡ David Braunstein, Benjamin R. Cowen, Mi Kyung Hong,§ Icko E. T. Iben,⊥ J. Bruce Johnson, Stan Luck, Michael C. Marden,‖ Judith R. Mourant, Pal Ormos,∫ Lou Reinisch,# Reinhard Scholl, Alfons Schulte,▽ Erramilli Shyamsunder,◆ Larry B. Sorensen,▲ Peter J. Steinbach, Aihua Xie, Robert D. Young,× and Kwok To Yue▼

Departments of Physics and Biophysics, University of Illinois at Urbana-Champaign, Urbana, Illinois 61801
(Received: July 12, 1989)

The exploration of the combined effects of pressure and temperature leads to new insights into the structure, dynamics, and reactions of proteins. A protein molecule possesses many conformational substates, nearly isoenergetic structures performing the same function but possibly with different rates. Pressure alters both the relative substate populations and the functional properties of the individual substates and thus can produce large changes in the static and dynamic properties of a protein ensemble. Such pressure effects have been measured for myoglobin (Mb), using visible and FTIR techniques. Above a glass temperature, T_{ig}, pressure redistributes substate populations and changes protein structure, the position of spectral bands, and protein reaction rates. Equilbrium substate populations measured from 230 to 330 K at pressures up to 200 MPa yield a thermodynamic comparison of different substates at pH 5.6 and 6.6. Near T_{ig}, pressure jump experiments reveal several relaxation processes. Well below T_{ig}, the properties of the proteins at temperature T and pressure P depend on history, i.e., on the order in which the sample is pressurized and cooled. The effect of pressure on the binding CO and O_2 to Mb after photodissociation points to the strong influence of conformational substates on protein reactions. Pressure controls the rate of binding through the activation volume and through redistribution of substate populations. The conformational effect of pressure differs for CO and O_2, and for sperm whale and horse myoglobin.

1. Introduction

The first draft of this paper was written 11 years ago. We did not publish then because we did not sufficiently understand the results, but we continued to explore the effects of pressure on protein states and reactions. During this time, Professor Harry Drickamer has been an unfailing advisor and friend who has helped us with the design of equipment, with overcoming many difficult problems, and most importantly by setting standards for scientific research. We now believe that we have come closer to comprehending the effect of pressure on proteins, and we use the occasion of the Drickamer Special Issue to summarize our work. Many collaborators have contributed during these past 11 years, explaining the length of the author list which would be more appropriate for a high-energy physics paper. The many years of work are responsible for the length of the paper.

Pressure is an important variable not only in chemistry and physics, but also in biology.[1] Pressure can deactivate enzymes, viruses, and toxins, kill bacteria and yeasts, reverse narcosis induced by alcohol, and influence bioluminescence.[2] Sharks function from sea level to extreme depth,[3,4] encountering pressures from 0.1 to 100 MPa.[5] In order to explain these biological phenomena on a molecular level, the effects of pressure on isolated proteins must be understood. Many pressure studies of proteins have been performed,[1,6,7] but usually in a narrow temperature range near 300 K. As we shall show, studies over a wide temperature range are needed for an interpretation of the observed pressure effects.

The effects of a pressure P on a protein can be explained with Figure 1 which gives two vastly simplified cross sections through the energy hypersurface of a protein. We assume that the protein has two conformations (or conformational substates) 0 and 1 (Figure 1a) and two states A and B (Figure 1b). In each of the two substates 0 and 1, the protein can make the transition B → A. Figure 1 shows in panel a the cross section through the energy surface at constant reaction coordinate, say rc = B. Panel b represents the cross section at constant conformational coordinate (say cc = 1). Pressure affects the protein characterized by Figure 1 in two ways. In *equilibrium*, the ratio w_0/w_1 of the populations w_0 and w_1 of the two conformational substates 0 and 1 at temperature T is given by

$$w_0/w_1 = \exp[-\Delta G/RT] \tag{1}$$

where ΔG is the difference in Gibbs free energy between the two substates,

$$\Delta G = \Delta E + P\,\Delta V - T\,\Delta S \tag{2}$$

Here ΔE, ΔV, and ΔS are the differences in internal energy, volume, and entropy between the two conformations. Pressure shifts the equilibrium ratio by the factor $\exp[-P\,\Delta V]$. Pressure also affects the *reaction rate*. If a reaction B → A occurs in the conformational substate i, the reaction rate coefficient k^i_{BA} can be written as

$$k^i_{BA} = \nu \exp(-G^*_{BA}/RT) \tag{3}$$

Here

$$G^*_{BA} = E^*_{BA} + PV^*_{BA} - TS^*_{BA} \tag{4}$$

is the activation Gibbs free energy and ν is the frequency factor in the substate i. The star indicates that G^* is ideally measured

† Current address: Department of Physics, Simon Fraser University, Burnaby, BC V5A 1S6 Canada.
‡ Current address: National Institutes of Health, 9000 Rockville Place, Bethesda, MD 20892.
§ Current address: Department of Physics, Princeton University, Princeton, NJ 08540.
⊥ Current address: AT&T Bell Labs., 600 Mountain Avenue, Murray Hill, NJ 07974.
‖ Current address: INSERM U.299, 78 Rue de General Leclerc, 94275 Le Kremlin Bicetre, France.
∫ Permanent address: Biophysics Institute, Hungarian Academy of Sciences, 6701 Szeged, Hungary.
Current address: USUHS/Laser Biophysics Center, Bethesda, MD 20814.
▽ Current address: IBM Almaden Research Center, 650 Harry Road, San Jose, CA 95120.
◆ Current address: Department of Physics, University of Washington, Seattle, WA 98195.
▲ Permanent address: Department of Physics, Illinois State University, Normal, IL 61761.
× Current address: Department of Physics, Emory University, Atlanta, GA 30322.

(1) Jannasch, H. W., Marquis, R. E., Zimmerman, A. M., Eds. *Current Perspectives in High Pressure Biology*; Academic: New York, 1987.
(2) Johnson, F. H., Eyring, H., Stover, B. J. *The Theory of Rate Processes in Biology and Medicine*; Wiley: New York, 1974.
(3) Regnard, P. *Recherches experimentales sur les conditions physiques de la vie dans les eaux*; Librarie de l'academie de Medecine: Paris, 1891.
(4) Isaacs, J. D., Schwartzlose, R. A. *Sci. Am.* **1975**, *4*, 84.
(5) 1 Pa = 1 pascal = 10^{-5} bar. 100 MPa = 1 kbar.
(6) Heremans, K. A. H. *Annu. Rev. Biophys. Bioeng.* **1982**, *11*, 1. Monkd, E. *Adv. Protein Chem.* **1981**, *34*, 93.
(7) Weber, G., Drickamer, H. G. Q. *Rev. Biophys.* **1983**, *16*, 1.

0022-3654/90/2094-1024$02.50/0

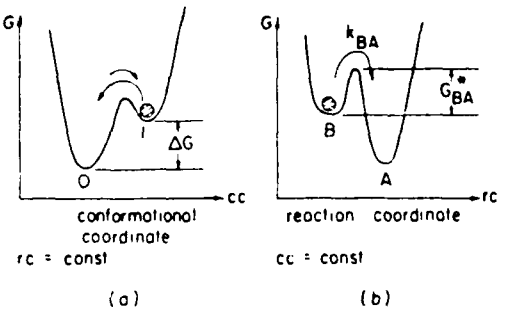

Figure 1. Two cross sections through a highly simplified energy hypersurface of a protein. (a) At constant reaction coordinate (e.g., B in panel b) the protein possesses two conformations 0 and 1. (b) At constant conformational coordinate (e.g., 0 in panel a) the protein possesses two states. The bullet represents the protein–ligand system.

at constant viscosity. The factor $\exp[-PV^*_{BA}/RT]$ can either speed up or slow down the reaction rate.

As we will discuss in more detail in section 2, a protein molecule in a given state does not exist in only one or two conformations but assumes a large number of conformational substates (CS)[8] which most likely are arranged in a hierarchy.[9] Substates are defined as having similar, but not identical, structure, and performing the same function, but possibly with different rates. As discussed above for the simplest case of two conformations, pressure can affect protein dynamics and reactions in two ways. Within a given CS, pressure can change a reaction rate according to eq 3 and 4; the change depends upon the activation volume V^*_{BA} which may be different in different CS. Equally importantly, however, pressure may shift the population from one substate to another. Since the different CS may have different reaction rates, pressure can change the overall reaction rate by a factor that cannot be described by an activation volume alone.

In the present paper we describe five pressure effects that are based on the eq 1–4 and on the fact that proteins possess conformational substates:

(i) Well above a characteristic temperature T_{sg}, defined in section 2, protein substates are in equilibrium. If the ratio of substate populations can be monitored as a function of pressure and temperature, then eq 1 and 2 permit a determination of the differences in energy, entropy, and volume between substates and thus yield a detailed thermodynamic description of the protein substates (section 4).

(ii) Well below T_{sg}, proteins are in a metastable state. The combined use of pressure and temperature proves the metastability (section 5).

(iii) Pressure shifts some spectral lines. These shifts are caused by elastic effects and by changes in the populations of the conformational substates (section 6).

(iv) Near T_{sg}, pressure jump experiments permit measurements of the transitions among various substates (section 7).

(v) The binding of small ligands such as CO and O_2 to heme proteins can be studied in detail by using flash photolysis. The exploration of this reaction as a function of T and P, monitored in the Soret (visible) and the infrared regions, shows that pressure indeed affects reaction rates both through the activation volume and through shifts in the substate populations (section 8).

2. Conformational Substates and Motions

2.1. Myoglobin. Myoglobin is a globular protein, built of 153 amino acids and with overall dimensions 4.5 × 3.5 × 2.5 nm³, that binds O_2 and CO reversibly.[10] In Figure 2, we sketch carbonmonoxymyoglobin (MbCO), with CO bound to the heme iron at an angle α with the heme normal.

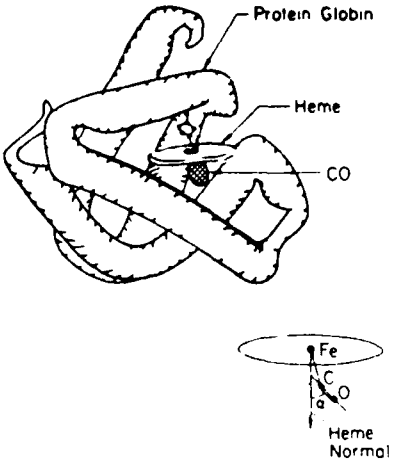

Figure 2. Schematic view of myoglobin with CO bound at the heme iron. The Fe and CO are shown enlarged. The CO dipole makes an angle α with the heme normal.

2.2. States, Substates, and Motions.[8,9] Most proteins perform some function such as catalysis or transport of matter or charge. They must consequently possess at least two *states*, for instance, Mb and MbO_2. Proteins in different states perform different functions (Mb binds and MbO_2 dissociates O_2) and may have different structures and properties. As stated in section 1, each state consists of a large number of *conformational substates* (CS). CS have somewhat different structures but perform the same function, albeit with different rates. All substates of Mb, for instance, bind CO, but with different association rates. Conformational substates are valleys in the energy hypersurface of a protein in a particular state.

The existence of states and substates leads to two different types of motions, *equilibrium fluctuations* (EF) and nonequilibrium transitions called *functionally important motions* (FIM).[9] EF are motions between CS in equilibrium, and FIM are the nonequilibrium motions that lead from one state (say Mb) to another (MbO_2). EF and FIM are connected by fluctuation–dissipation theorems.

2.3. Hierarchy of Substates.[9,11] In MbCO, experiments suggest a hierarchical arrangement of CS as shown schematically in Figure 3, where the conformational energy of MbCO is plotted as a function of multidimensional conformational coordinates (cc). In principle, listing the coordinates of all atoms in a given protein molecule describes a CS completely. Figure 3 indicates that the substates in MbCO are arranged in tiers, with tier 0 having the largest barriers between energy valleys. The evidence for tiers in MbCO is as follows:

Tier 0 (CS^0). Evidence for the substates in tier 0 comes from the stretch frequency ν_{CO} of the CO bound to Mb, shown in Figure 4.[11] The IR spectrum shows three major resolvable stretch bands which we denote by A_0 ($\nu_{CO} \approx 1966$ cm^{-1}), A_1 ($\nu_{CO} \approx 1945$ cm^{-1}), and A_3 ($\nu_{CO} \approx 1933$ cm^{-1}). The three bands correspond to three substates; they have approximately the same structure but differ in detail as indicated by the values of the tilt angle α between the bound CO and the heme normal: $\alpha(A_0) = 15 \pm 3°$, $\alpha(A_1) = 28 \pm 2°$, $\alpha(A_3) = 33 \pm 4°$.[12,13] The three substates perform the same function—binding of CO—but with different rates; A_0 rebinds fastest and A_3 slowest.[11]

Tier 1 (CS^1). Rebinding of CO to each CS^0 is nonexponential in time, as proven in ref 11 and also shown later in section 8. The simplest explanation for the nonexponential rebinding is the ex-

(8) Frauenfelder, H.; Parak, F.; Young, R. D. *Annu. Rev. Biophys. Biophys. Chem.* **1988**, *17*, 451.
(9) Ansari, A.; Berendzen, J.; Bowne, S. F.; Frauenfelder, H.; Iben, I. E. T.; Sauke, T. B.; Shyamsunder, E.; Young, R. D. *Proc. Natl. Acad. Sci. USA* **1985**, *82*, 5000.
(10) Stryer, L. *Biochemistry*, 3rd ed.; Freeman: New York, 1988.
(11) Ansari, A.; Berendzen, J.; Braunstein, D.; Cowen, B. R.; Frauenfelder, H.; Hong, M. K.; Iben, I. E. T.; Johnson, J. B.; Ormos, P.; Sauke, T. B.; Scholl, R.; Schulte, A.; Steinbach, P. J.; Vittitow, J.; Young, R. D. *Biophys. Chem.* **1987**, *26*, 337.
(12) Ormos, P.; Braunstein, D.; Frauenfelder, H.; Hong, M. K.; Lin, S. L.; Sauke, T. B.; Young, R. D. *Proc. Natl. Acad. Sci. USA* **1988**, *85*, 8492.
(13) Moore, J.; Hansen, P.; Hochstrasser, R. *Proc. Natl. Acad. Sci. USA* **1988**, *85*, 5062.

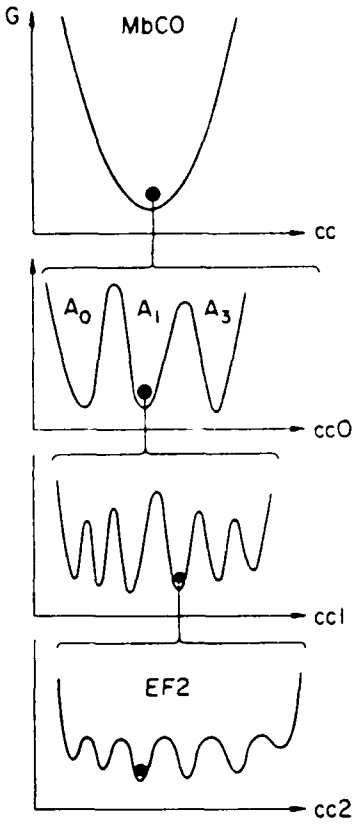

Figure 3. Hierarchical arrangement of the conformational substates in MbCO. The diagram represents a one-dimensional cross section through the multidimensional conformational energy surface of MbCO. Three tiers of substates (CS^i, i = 0, 1, 2) are shown as functions of three conformational coordinates (cc$i$, i = 0, 1, 2). MbCO can exist in three substates of tier 0. Each of these can assume a large number of conformations corresponding to substates of tier 1. The furcation continues at least through tier 2.

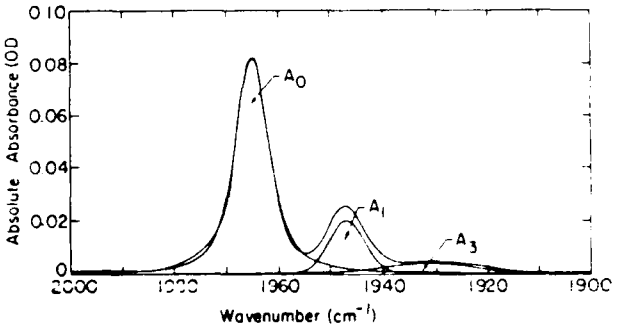

Figure 4. The IR spectrum of swMbCO fit to three Voigtians corresponding to three A bands. The spectrum shown is for a sample cooled to 25 K and then pressurized to 200 MPa, pH = 5.5. Solvent: 75% glycerol/water (v/v).

istence of CS.[14,15] Since each CS^0 separately displays nonexponential behavior, each CS^0 must be furcated into a large number of substates, which are therefore called CS^1. The nonexponential time dependence of rebinding proves that the different CS^1 rebind with different rates.

Tier 2 (CS^2). Originally we postulated the existence of substates CS^2 within the CS^1 because of a shift of the near-IR band at 760 nm after photodissociation of MbCO.[9] Agmon[16] and Campbell et al.[17] have shown, however, that the major contribution to the shift is due to a narrowing of the inhomogeneously broadened line during the course of CO rebinding. Nevertheless, independent evidence for CS^2 comes from the Mössbauer effect[18] and from pumping experiments.[11,19,20] The pumping results imply that different CS^2 within a given CS^1 rebind CO with different rates.

It is likely that substates (CS^3, CS^4) within CS^2 exist,[9] but they are not important for the present work.

2.4. Slaved Glass Transitions. Around 300 K, equilibrium fluctuations (EF0, EF1, ...) occur in all tiers. As the temperature is lowered, EF in successive tiers freeze out. As we have proven earlier[11,21] and will show in sections 4 and 7, the exchange between the substates of tier 0 stops near 180 K and that between the substates of tier 1 near 160 K. The freezing of these two tiers is similar to a glass transition, but with one difference: The transition temperatures depend on the solvent. We call such a transition "slaved"[11,21] and denote the transition temperature as T_{ig}. Slaving is most pronounced for tier 1, where the transition in the protein occurs very close to that of the glass temperature of the solvent. Less is known about the transitions in tier 2, but preliminary data indicate that tier 2 freezes out gradually and slow exchange may take place even at 60 K.

2.5. Substates and Pressure. The relevance of conformational substates to the design and interpretation of pressure experiments is now clear for the binding of CO or O_2 to Mb. Since different substates in each tier rebind ligands with different rates, a switch in population caused by pressure affects the overall binding rate of the protein ensemble. Pressure experiments consequently help explore protein dynamics in two different directions. They provide information about ligand binding and about the hierarchy of CS. In discussing these effects, the role of temperature is crucial. Depending on the tier, temperature, and reaction or observation time, the system either remains frozen in a particular substate or moves from CS to CS. In the frozen ensemble, the reaction proceeds nonexponentially in time; if the exchange between substates is rapid compared to the reaction, it shows an exponential time dependence.[14]

3. Experimental Methods

Here we describe the experimental tools used for the five types of pressure studies listed in the introduction. The experiments involve three types of measurements: the observation of the stable and metastable states of MbCO in the Soret and IR regions as functions of pressure and temperature, the observation of IR spectra as functions of time after a pressure change, and observation of the time dependence of rebinding of CO and O_2 after flash photolysis as functions of temperature and pressure in the Soret and IR regions.

Lyophilized metmyoglobin powders from sperm whale (sw) and horse (h) were purchased from Sigma Chemical Co. Myoglobin solutions were prepared by dissolving metMb in 75% (v/v) glycerol/buffer and adding excess sodium dithionite. The samples near pH 7 were buffered with 0.1 M potassium phosphate while those near pH 5 were buffered with 0.3 M potassium citrate. The pH of each IR sample was measured after protein was added.

The pressure cell has evolved through several versions over 10 years. Here we describe the latest design with which all the IR spectra were taken (Figure 5). The pressure cell is constructed of beryllium–copper with two sapphire windows for Soret and infrared measurements. The windows are held in place on mushroom plugs using a modified "unsupported area" seal which

(14) Austin, R. H.; Beeson, K. W.; Eisenstein, L.; Frauenfelder, H.; Gunsalus, I. C. *Biochemistry* **1975**, *14*, 5355.

(15) Frauenfelder, H. In *Structure and Dynamics: Nucleic Acids and Proteins*; Clementi, E., Sarma, R. H., Eds.; Adenine: Guilderland, 1983, p 269.

(16) Agmon, N. *Biochemistry* **1988**, *27*, 3507.

(17) Campbell, B. F.; Chance, M. R., Friedman, J. M. *Science* **1987**, *238*, 373.

(18) Frauenfelder, H., in *Structure and Motion: Membranes, Nucleic Acids, and Proteins*. Clementi, E., Corongiu, G., Sarma, M. H., Sarma, R. H. Eds. Adenine: Guilderland, NY, 1985, p 205.

(19) Sauke, T. B. Ph.D. Thesis, University of Illinois at Urbana–Champaign, 1989.

(20) Sauke, T. B., Frauenfelder, H., Luck, S., Steinbach, P. J., Xie, A., Young, R. D. *Biophys. J.* **1989**, *55*, 565a.

(21) Iben, I. E. T., Braunstein, D., Doster, W., Frauenfelder, H., Hong, M. K., Johnson, J. B., Luck, S., Ormos, P., Schulte, A., Steinbach, P. J., Xie, A. H., Young, R. D. *Phys. Rev. Lett.* **1989**, *62*, 1916.

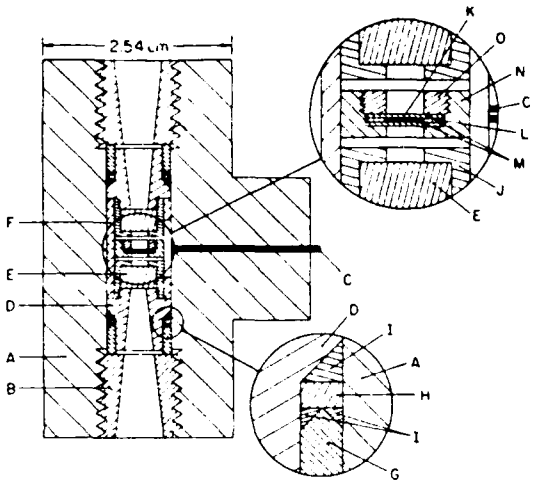

Figure 5. The high-pressure infrared cell. The cell has been used at temperatures between 10 and 350 K, and at pressure up to 400 MPa. All parts are made of beryllium–copper unless otherwise indicated. The parts are as follows: (A) cell body; (B) threaded window support plug; (C) stainless steel high-pressure tubing hard soldered to cell body (0.78 mm outer diameter, 0.15 mm inner diameter); (D) window support; (E) sapphire window; (F) core tube; (G) support ring; (H) indium packing; (I) brass antiextrusion rings; (J) window cap; (K) protein sample; (L) Mylar spacer; (M) sapphire windows; (N) sample cell; and (O) sample cell bottom.

withstands helium gas pressure up to 400 MPa at temperatures from 40 to 350 K. The pressurizing gas enters the cell through 60 cm of coiled stainless steel tubing (OD 0.78 mm, ID 0.15 mm) enclosed within the vacuum chamber to minimize heat conduction along the tubing. The MbCO sample is contained between two sapphire windows (0.25 mm thick) within a thin doughnut-shaped Mylar spacer (0.075, 0.125, or 0.175 mm). The sample, sapphire windows, and Mylar spacer are held together by a beryllium–copper sample holder which fits inside the pressure cell.

Helium gas is pressurized by using a Harwood Engineering A2.5J Intensifier or an Aminco (now Superpressure) compressor (Model 46-14060) after being filtered by a 5-μm filter. The pressure is monitored with a Bourdon gauge accurate to within 4 MPa.

The static absorption spectra in the Soret region were taken with a Cary-14 spectrometer. The myoglobin concentration was about 15 μM and the path length was about 7 mm.

The ligand rebinding measurements in the Soret region were obtained with a flash photolysis system.[40] The photolysis pulse was generated by a flashlamp-pumped dye laser (Phase-R DL-1000) using coumarin 6 dye (540 nm, 100–150 mJ). Rebinding was monitored with light from a tungsten lamp passed through an interference filter and collected onto a photomultiplier (RCA 4837). The photomultiplier output from 2 μs to 300 s was digitized with a logarithmic time-base digitizer. The pressure cell containing the sample was placed in a liquid helium storage Dewar (Janis), and the temperature was monitored with a Si diode on the pressure cell. The protein concentrations for the Soret flash photolysis measurements were 220 μM for MbCO and 300 μM for MbO_2; the sample path length was 0.5 mm.

The IR spectra were taken on a Mattson Sirius 100 FTIR spectrometer at 2 cm^{-1} resolution. Low temperatures were maintained with a closed-cycle helium refrigerator (CTI Model 22C) and a Lake Shore Cryogenics temperature controller (Model 93C). A silicon diode mounted on the sample cell monitored the temperature. Photolysis for the IR rebinding experiments was achieved with an argon ion laser operating at 514 nm with an intensity of 0.4 W/cm^2 and a beam diameter of about 3 mm. The pH 6.6 samples were 15 mM MbCO, and were photolyzed for 20 s; the pH 5.5 samples were 5 mM MbCO and were photolyzed for 10 s. All samples used for flash photolysis were 0.075 mm thick. Absolute absorbance spectra (as in Figure 9) were obtained by subtracting either a solvent background or a solvent deoxymyoglobin background from the MbCO spectrum. Sperm whale myoglobin was used for all IR samples.

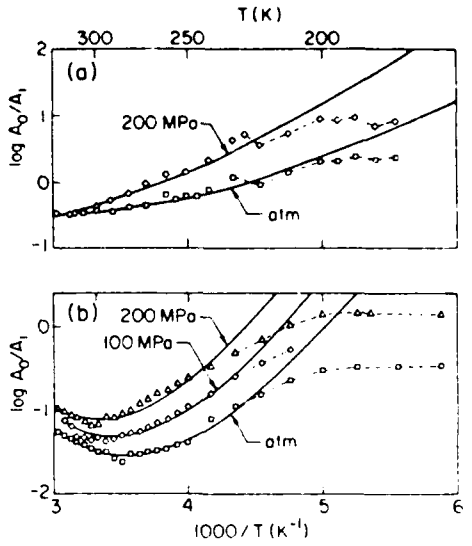

Figure 6. Logarithm of the ratio of areas, A_0/A_1, of CO stretch bands, at pH 5.5 (a) and pH 6.6 (b), as a function of $1000/T$ for different pressures. Sample: swMbCO in 75% glycerol/water (v/v).

The CO stretch bands were fit in a two-step process. First, the base line was fit to a cubic polynomial by a standard linear least-squares method. Then, the bands were fit to Voigtian line shapes (Gaussian superpositions of Lorentzians) by using a finite difference Levenberg–Marquardt nonlinear least-squares algorithm. The spectra were fit to four Voigtians to account for the asymmetry of A_0 at pH 5.5 and of A_1 at pH 6.6.

4. Equilibrium Properties

The behavior of the substates of tier 0 as a function of P and T is shown in Figure 6, where the ratios of the areas of the CO stretch bands of swMbCO, for two pH values, are plotted vs $1000/T$ for different pressures. Above about 330 K MbCO unfolds, and the entire CO stretch spectrum changes. Between about 330 and 200 K, the three A substates are in equilibrium. In the transition region between about 200 and 180 K, exchange between the A substates becomes measurably slow. Below about 180 K, the exchange is immeasurably slow and each protein molecule remains frozen into a particular CS^0; the protein has become glasslike. We use the terms glassy or glasslike to describe a frozen and metastable complex system. In the present section, we treat the equilibrium region.

The equilibrium region of A_0/A_1 shows two van't Hoff-like parts, with a minimum near 300 K. We have shown that for constant pressure this behavior follows from the thermodynamic properties of proteins.[22] Here we generalize the treatment to include pressure and show that the data in Figure 6 lead to a determination of the relative thermodynamic parameters of the A substates.

We assume that the A substates have equal extinction coefficients.[23] The ratio of the populations of the substates in eq 1 is then equal to the ratio of the band areas. If the thermodynamic parameters E, V, and S are taken to be independent of T, the data in Figure 6 cannot be fit with only the two substates A_0 and A_1. Experiments show, however, that the specific heat of globular proteins is essentially linear from 200 to 320 K.[24] The entropy can consequently be approximated by $S(T) = S(0) + sT$. We generalize this expression to also include a term linear in pressure

$$S(T,P) = S(0) + sT + vP \qquad (5)$$

(22) Hong, M. K.; Braunstein, D.; Cowen, B. R.; Frauenfelder, H.; Iben, I. E. T.; Mourant, J. R.; Ormos, P.; Scholl, R.; Schulte, A.; Steinbach, P. J.; Xie, A. H.; Young, R. D. *Biophys. J.*, submitted for publication.

(23) Morikis, A.; Champion, P. M.; Springer, B. A.; Sligar, S. G. *Biochemistry* **1989**, *28*, 4791.

(24) Mrevlishvili, G. M. *Sov. Phys. Usp.* **1979**, *22*, 433.

TABLE I: Thermodynamic Parameters for the Population Ratios A_0/A_1 at pH 6.6 and 5.5[a]

parameter	pH 6.6	pH 5.5
$\Delta E(0)$, kJ mol^{-1}	−68	−22
$\Delta V(0)$, cm^3 mol^{-1}	−45	−42
$\Delta S(0)$, J mol^{-1} K^{-1}	−510	−150
Δv, cm^3 mol^{-1} K^{-1}	−0.11	−0.13
Δs, J mol^{-1} K^{-2}	+1.7	+0.44

[a] Data and fit shown in Figure 6. Errors are ±25%. Sample: swMbCO in 75% glycerol/water (v/v).

This expansion is justified by noting that the Maxwell relation $(\partial S/\partial P)_T = -(\partial V/\partial T)_P$ yields

$$V(T,P) = V(0) - vT \tag{6}$$

With

$$v = -\beta V(0) \tag{7}$$

eq 6 is the standard relation $V(T) = V(0)(1 + \beta T)$, where β is the coefficient of thermal expansion and where the compressibility has been neglected. From eq 5, standard thermodynamics yields

$$E(T,P) = E(0) + vPT + \tfrac{1}{2}sT^2 \tag{8}$$

The difference in Gibbs free energy between substates A_0 and A_1 becomes

$$\Delta G(T,P) \equiv G_0 - G_1 = \Delta E(0) + P\,\Delta V(0) - T\,\Delta S(0) - \Delta vPT - \tfrac{1}{2}\Delta sT^2 \tag{9}$$

where, for instance, $\Delta E(0) \equiv E_0(0) - E_1(0)$, and $E_0(0)$ is the internal energy of substate A_0 at $T = 0$, $P = 0$.

Fits to eq 1 and 9 yield the solid lines in Figure 6 and the parameters in Table I. These values, together with eq 5, 6, and 8, give the differences in entropy (in units of R), energy, and volume between substates as a function of temperature shown in Figure 7.

In order to discuss the results in Table I and Figure 7 we first note that the volume differences are given in cm^3/mol, with 1 cm^3/mol = 1.67×10^{-3} nm^3/molecule = 1.67 Å^3/molecule. The volume V_{Mb} of a Mb molecule is about 40 000 Å^3. The pocket volume is about 200 Å^3. The ratios $\Delta V/V_{Mb}$ are of the order of 10^{-3}, indicating that the overall volumes of the three substates are nearly the same. The volume of A_0 is smallest, but the difference ΔV decreases with increasing temperature. Below about 300 K, A_0 also has the smallest entropy and the lowest internal energy. This observation suggests that A_0 may be stabilized by additional hydrogen bonds at low T and that the number of these bonds decreases with increasing T. X-ray diffraction studies at different pH and pressures[25,26] and calorimetric studies at different pH are needed to explore the substates in more detail.

A last remark here concerns the value of v. With eq 7 we write

$$\Delta v = -\Delta[\beta V(0)] \approx -\beta\Delta V(0) - V(0)\Delta\beta \tag{10}$$

Using $\Delta V(0)$ from Table I and taking the volume thermal expansion coefficient β from X-ray data[27] as 3.5×10^{-4} K^{-1} gives for the first term in eq 10 the value +0.01 cm^3/(mol K). Since Δv for A_0 is negative, the main contribution to Δv must come from the second term, suggesting that $\Delta\beta/\beta \approx \Delta v/\beta V(0) = \Delta v/\beta V_{Mb} \approx 0.005$.

5. The Metastable Glass State

Below about 160 K, the exchange among substates of tier 0 and tier 1 is frozen, and the protein is glasslike.[21,28-33] Two outstanding characteristics of the glassy (amorphous) state are a rugged energy landscape and metastability. The rugged energy landscape, valleys within valleys within valleys, is shown in Figure 3. Metastability implies that the state of the system below the glass temperature depends on its history and that the system is trapped in a substate with an energy above the lowest energy. History dependence can be shown by moving in the TP plane (Figure 8) from a point above the glass transition to a point below T_{sg} by two different pathways.[34] In equilibrium, the properties

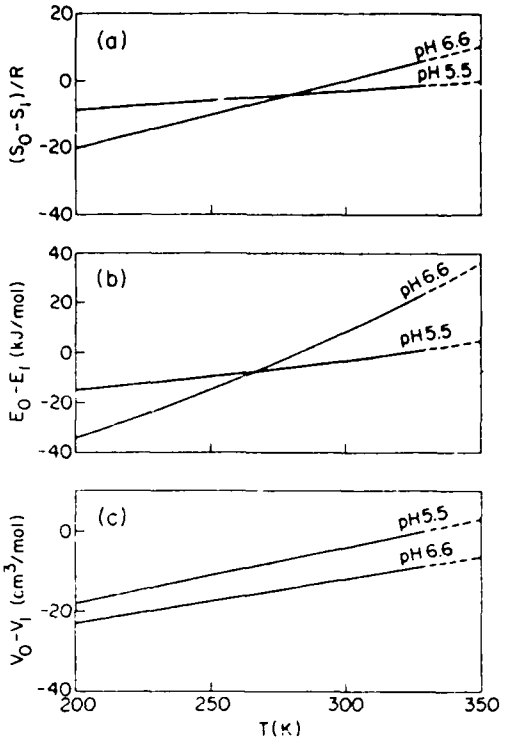

Figure 7. Differences in entropy (in units of R), energy (kJ/mol), and volume (cm^3/mol) between the substates A_0 and A_1 at pH 6.6 and pH 5.5 at zero pressure as a function of temperature. The differences are derived from the fits in Figure 6.

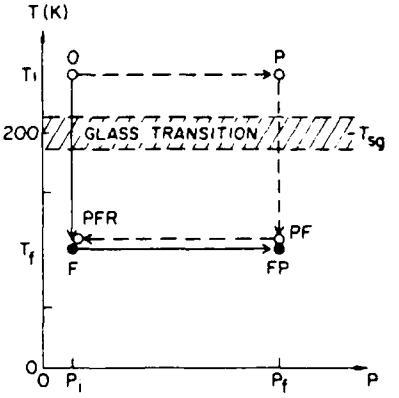

Figure 8. The protein sample is taken from an initial state (T_i,P_i) to a final state (T_f,P_f) on different pathways, for instance O → F → FP (solid path) and O → P → PF (dashed path). In equilibrium, the protein properties in the two states must be identical. Metastability is proven if different properties are found at FP and PF.

(25) Kuriyan, J.; Wilz, S.; Karplus, M.; Petsko, G. A. *J. Mol. Biol.* **1986**, *192*, 133.
(26) Tilton, Jr., R. F.; Petsko, G. A. *Biochemistry* **1988**, *27*, 6574.
(27) Frauenfelder, H.; Hartmann, H.; Karplus, M.; Kuntz, Jr., I. D.; Kuriyan, J.; Parak, F.; Petsko, G. A.; Ringe, D.; Tilton, Jr., R. F.; Connolly, M. L.; Max, N. *Biochemistry* **1987**, *26*, 254.
(28) Frauenfelder, H.; Petsko, G. A.; Tsernoglou, D. *Nature* **1979**, *280*, 558.
(29) Goldanskii, V. I.; Krupyanskii, Yu. F.; Fleurov, V. N. *Dokl. Akad. Nauk. SSSR* **1983**, *272*, 978.
(30) Singh, G. P.; Schink, H. J.; von Löhneysen, H.; Parak, F.; Hunklinger, S. *Z. Phys.* **1984**, *B55*, 23.
(31) Champion, P. M.; Sievers, A. J. *J. Chem. Phys.* **1980**, *72*, 1569.
(32) Morozov, V. N.; Gevorkian,S. G. *Biopolymers* **1985**, *24*, 1785.
(33) Doster, W., Bachleitner, A.; Dunan, R.; Hiebl, D.; Lüscher, E. *Biophys. J.* **1986**, *50*, 213.
(34) Eisenstein, L.; Frauenfelder, H. In *Frontiers of Biological Energetics*; Academic Press: New York, 1978; Vol. 1, p 280.

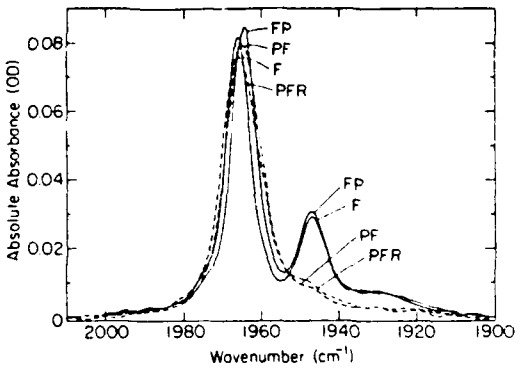

Figure 9. The MbCO stretch spectrum determined at the points F, FP, PF, PFR in the TP plane of Figure 8, with T_i = 225 K, T_f = 100 K, P_i = 0.1 MPa, and P_f = 200 MPa. In equilibrium, the pairs F/PFR, and FP/PF should yield identical spectra. The different spectra prove metastability. Sample: swMbCO in 75% glycerol/water (v/v) at pH 5.5.

of the system are independent of the path (history). For most of our experiments we select the two pathways shown in Figure 8. On the solid pathway, we freeze the sample (F) and then pressurize (FP). On the dashed pathway, we first pressurize (P), then freeze (PF), and finally release the pressure (PFR). In equilibrium, F and PFR or FP and PF should yield identical protein properties. Figure 9 shows the results of such an experiment, where the CO stretch spectrum of swMbCO is measured at the four points F, FP, PF, PFR in the TP plane, with T_i = 225 K, T_f = 100 K, P_i = 0.1 MPa, P_f = 200 MPa. The infrared spectra obtained via the two pathways differ considerably: Metastability is proven.

6. Pressure Effects on Spectral Lines

6.1. Elastic and Conformational Pressure Effects. In crystals, the dominant effect of a moderate pressure on the optical spectra is a peak shift, usually to lower wavenumber (red shift). The pressure compresses the crystal and decreases the distances between the atoms, thereby changing the total energy. The arrangement (topology) of the atoms remains unchanged. Since this effect involves only an elastic deformation of the crystal, it occurs rapidly at any temperature. At the pressures of interest here ($P \leq 200$ MPa), the wave number shift $\delta\nu_e$ is linear in P

$$\delta\nu_e = c_e P \tag{11}$$

and the coefficient c_e is proportional to the volume difference between the ground and the excited state of the optical transition.[35]

In proteins, the situation is more complex and two different types of pressure effects occur, elastic and conformational (plastic).[36] The *elastic* effect is similar to the one in crystals: The protein remains in the same substate and does not change conformation, and the arrangement (topology) of the atoms remains unchanged. The spectral shift is due to an increase in the density and hence energy of the protein. The *conformational* effect is characteristic of proteins, but is similar to the effect of pressure on thermal transitions discussed by Drickamer and co-workers.[37] In conformational effects, pressure changes the local or global arrangement of the atoms; the protein moves from one conformational substate to another. Each conformational substate may give rise to a line with a slightly different peak wavenumber, and the overall band may be a Gaussian superposition of Lorentzians (Voigtian). Thus, spectral lines in proteins are inhomogeneously broadened:[16,17,38,39] a pressure-induced shift in the substate populations not only shifts the line but also changes its shape.

(35) Slichter, C. P.; Drickamer, H. G. *Phys. Rev. B* **1980**, *22*, 4097.
(36) Noguti, T.; Go, N. *Proteins* **1989**, *5*, 97.
(37) Drickamer, H. G.; Frank, C. W.; Slichter, C. P. *Proc. Natl. Acad. Sci. USA* **1972**, *69*, 933.
(38) Agmon, N.; Hopfield, J. J. *J. Chem. Phys.* **1983**, *79*, 2042.
(39) Ormos, P.; Ansari, A.; Braunstein, D.; Cowen, B. R.; Frauenfelder, H.; Hong, M. K.; Iben, I. E. T.; Sauke, T. B.; Steinbach, P. J.; Young, R. D. *Biophys. J.*, in press.

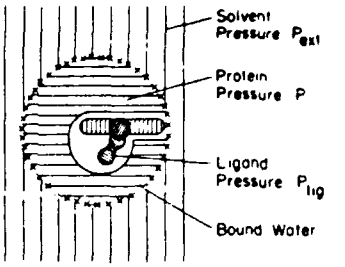

Figure 10. Pressure screening. An externally applied pressure P_{ext} may not be fully transmitted to the protein. The pressure seen by the protein is given by $P = qP_{ext}$. The ligand bound at the heme may be additionally shielded by the heme pocket so P_{lig}, the pressure the ligand feels, may differ from P.

Elastic and conformational band shifts can be distinguished with the technique depicted in Figure 8: At the temperature T_i ($> T_{sg}$) both the elastic and the conformational shifts occur. At T_f ($\ll T_{sg}$), only the elastic shift takes place. To discuss these shifts, we consider the simplest case and assume two conformational substates (Figure 1a), with peak wavenumbers ν_0 and ν_1 and elastic shifts $\delta\nu_0$ and $\delta\nu_1$. We further assume the normalized populations $w_0(P)$ and $w_1(P)$ of the two substates to be functions of pressure. The average wavenumbers in the four pressure states of Figure 8 then become

$$\begin{aligned}
\nu_F &= w_0(0)\nu_0 + w_1(0)\nu_1 \\
\nu_{FP} &= w_0(0)(\nu_0 + \delta\nu_0) + w_1(0)(\nu_1 + \delta\nu_1) \\
\nu_{PF} &= w_0(P)(\nu_0 + \delta\nu_0) + w_1(P)(\nu_1 + \delta\nu_1) \\
\nu_{PFR} &= w_0(P)\nu_0 + w_1(P)\nu_1
\end{aligned} \tag{12}$$

From these four observables we form, with $w_0(P) + w_1(P) = 1$, three independent differences

$$\begin{aligned}
\Delta_1 &\equiv \nu_{FP} - \nu_F = w_0(0)\delta\nu_0 + w_1(0)\delta\nu_1 \\
\Delta_2 &\equiv \nu_{PF} - \nu_{PFR} = w_0(P)\delta\nu_0 + w_1(P)\delta\nu_1 \\
\Delta_3 &\equiv \nu_{PFR} - \nu_F = [w_1(P) - w_1(0)][\nu_1 - \nu_0]
\end{aligned} \tag{13}$$

The first two differences are elastic, and they vanish if no elastic shift occurs; i.e., if $\delta\nu_0 = \delta\nu_1 = 0$. The third difference is conformational and is nonzero only if the pressure changes the population of the substates and the wavenumbers of the substates differ. Finally, a nonvanishing difference between Δ_1 and Δ_2

$$\Delta_2 - \Delta_1 = [w_1(P) - w_1(0)][\delta\nu_1 - \delta\nu_0] \tag{14}$$

proves that even the elastic shifts in the different substates differ.

6.2. Pressure Screening. In a crystal, the pressure inside is the same as the externally applied hydrostatic pressure P_{ext}. In a protein, the situation is more intricate as indicated in Figure 10. Two effects must be taken into account: In the glassy state below the glass temperature, T_g, of the solvent, the solvent may not transmit the entire pressure to the protein. At all temperatures, the ligand within the pocket may be shielded even from the protein pressure P by the pocket.

In a simple static model, where the coefficients of thermal expansion are neglected, the effective pressure at the protein can be calculated.[40] The resulting effective pressures in the four states below T_{sg} (Figure 8) are

$$P_F \approx 0,\ P_{FP} \approx qP_{ext},\ P_{PF} \approx P_{ext},\ P_{PFR} \approx (1 - q)P_{ext} \tag{15}$$

where

$$q = \frac{1 + (4/3)\mu_s\kappa_s}{1 + (4/3)\mu_s\kappa_p} \tag{16}$$

Here μ_s is the shear modulus of the solvent, and κ_s and κ_p are the compressibilities of the solvent and the protein. Protein com-

(40) Sorensen, L. B. Ph.D. Thesis, University of Illinois at Urbana-Champaign, 1980.

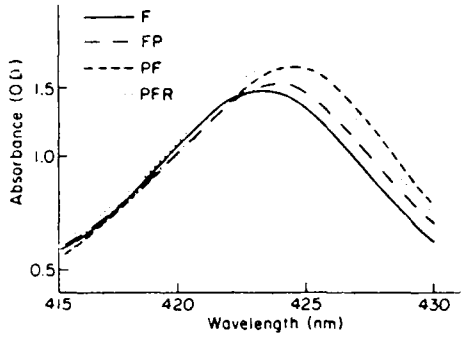

Figure 11. The Soret band for different pressure states. Sample: swMbCO in 75% glycerol/water solvent by volume, pH 7. T = 140 K, P = 190 MPa.

TABLE II: Peak Position of the Soret Band for swMb in the Pressure States Shown in Figure 8[a]

protein	T, K	solvent	peak position, nm F	FP	PF	PFR
MbCO	140	water	423.7	424.4	424.4	423.5
MbCO	140	75% G	423.4	423.8	424.5	423.8
MbCO	140	97% G	423.5	424.1	424.4	423.5
MetMb	120	75% G	410.0	410.7	411.3	410.2

[a] Pressure at P is 190 MPa. G denotes glycerol, % by volume. 50 mM phosphate buffer, pH 7. Points F, FP, PF, and PFR are explained in Figure 8.

pressibilites have been measured by using sound velocity[41,42] and fluorescence[43] techniques. The sound velocity technique measures an average value, the fluorescence experiment, a change in distance between the heme and a tryptophan residue. Since the distance can also be changed by a pressure-induced change in substates, and since q in eq 16 refers to an average protein value, we use the results from the sound velocity experiments. Some of the data in the next subsection refer to ice as the solvent. The relevant coefficients for ice are[44] μ_s = 3.8 GPa and κ_s = 0.11 GPa^{-1}; the compressibility of Mb lies between 0.06 and 0.12 GPa^{-1}. For ice as the solvent, q lies between 1.2 and 0.97. For the following discussions we assume q = 1.

We will see below that there exists evidence for additional screening of the CO molecule bound to the heme iron. The screening depends markedly on substate. To interpret the screening, X-ray structures for the different CS^0 will be required.

Differences in the thermal expansion of the protein and the solvent can also induce a pressure on the protein.[40] If the thermal expansion coefficient of the protein is smaller than that of the solvent, a temperature change may lead to tension, cancelling part of the external pressure. The experiments that will be discussed in section 8 indicate that this effect is not pronounced.

6.3. Pressure Shift of the Soret Band. A pressure-induced red shift of the Soret band in heme proteins has been observed by a number of groups.[45-47] Since these experiments were performed in a small temperature range, they do not provide information on the separation of the shift into elastic and conformational components.

We have measured the Soret band of swMb in a number of solvents at the four points F, FP, PF, and PFR of Figure 8. One set of data is shown in Figure 11, and the peak wavelengths in a few solvents are listed in Table II. For example, the values for swMbCO in a 75% glycerol–water solvent (Figure 11) give

TABLE III: Wavenumber Differences for the Stretch Bands A_0 and A_1 of swMbCO[a]

substate	pH	T, K	elastic shifts, cm^{-1} Δ_1	Δ_2	conformational shifts, cm^{-1} Δ_3	$\Delta_2 - \Delta_1$
A_0	5.5	25-100[b]	-1.6	-0.7	-0.2	+0.9
	6.6	50	-1.3	-0.5	-1.4	+0.8
A_1	5.5	25-100[b]	0			
	6.6	50	0	-0.1	+0.3	-0.1

[a] Differences are given in cm^{-1}, errors ±0.2 cm^{-1}. Pressure 200 MPa. 75% glycerol/water (v/v). Potassium phosphate buffer. The points F, FP, PF, and PFR are explained in Figure 8. [b] Average values.

the following with eq 13 and 14 and with $-\Delta\lambda/\lambda = \Delta\nu/\nu$: Δ_1 = -20 cm^{-1}; Δ_2 = -40 cm^{-1}, Δ_3 = -20 cm^{-1}, $\Delta_2 - \Delta_1$ = -20 cm^{-1}. The nonzero values of Δ_1 and Δ_2 prove that elastic shifts occur in the conformations between P = 0 and P = 190 MPa. The third difference implies that pressure changes the populations and that the peak wavenumbers of the substates are different. The finite value of $\Delta_2 - \Delta_1$ demonstrates that the elastic shifts in various substates are different.

The shifts for MbCO in 75% glycerol/water have been measured in the temperature range from 60 to 160 K and were found to be independent of T. This independence implies that the pressure effects caused by thermal expansion are small.

The pressure effect on the Soret band does not determine in which tier of substates the pressure effect occurs. This information can be obtained from pressure studies of the CO stretch bands in MbCO.

6.4. Pressure Effects on the CO Stretch Bands. Studies of the stretch vibrations in condensed systems by Drickamer and collaborators[48,49] show that ν_{CO} red shifts with increasing pressure; the coefficient c_e in eq 11 is of the order of 3×10^{-2} cm^{-1} MPa^{-1}. We have studied the effect of pressure on the stretch bands A_0 and A_1 of swMbCO. An example is shown in Figure 9. Apart from the change in population already discussed in section 4, pressure shifts the stretch bands and changes their shape. The shifts and shape changes depend on the path in the TP plane. In Table III we list the wavenumber differences as defined in eq 13 and 14 for the two bands A_0 and A_1 at two different pH values.

The two substates A_0 and A_1 are surprisingly different. A_1 shows very small or vanishing elastic and conformational shifts. A_0, in contrast, displays both elastic and conformational shifts. Even for A_0, however, the coefficient c_e in eq 11, $c_e \approx 5 \times 10^{-3}$ cm^{-1} MPa^{-1}, is considerably smaller than for carbonyls in liquids. The smallness of the elastic shifts and the different behavior of A_0 and A_1 may be caused by different pressure screening or by a different dielectric environment within the heme pocket. The Kirkwood–Bauer–Magat relation[50] gives for the elastic shift

$$\frac{\delta\nu_e}{\nu} = \text{const} \times \frac{\epsilon - 1}{2\epsilon + 1} \qquad (17)$$

where ϵ is the dielectric coefficient of the medium surrounding the CO dipole. Different ϵ may account for the magnitudes and differences of the elastic shifts.

The conformational pressure shift of A_0 implies that the substates of tier 1 within a given CS^0 have properties different enough to produce a conformational shift. This conclusion is supported by three more observations: The substate A_0 broadens under pressure as shown in Figure 9, the tilt angle α between the CO axis and the heme normal in a given CS^0 is distributed about its average value,[12] and different parts within a given CO stretch band rebind CO after photodissociation with different rates.[39]

7. Pressure Studies of Protein Dynamics

So far we have discussed the application of pressure to the study of protein structure, equilibrium behavior, and metastability.

(41) Gekko, K.; Noguchi, H. *J. Phys. Chem.* **1979**, *83*, 2706.
(42) Gavish, B.; Gratton, E.; Hardy, C. J. *Proc. Natl. Acad. Sci. USA* **1983**, *80*, 750.
(43) Marden, M. C.; Hui Bon Hoa, G.; Stetzkowski-Marden, F. *Biophys. J.* **1986**, *49*, 619.
(44) Hobbs, P. V. *Ice Physics*; Oxford: London, 1974.
(45) Ogunmola, G. B.; Zipp, A.; Chen, F.; Kauzmann, W. *Proc. Natl. Acad. Sci. USA* **1977**, *74*, 1.
(46) Gibson, Q. H.; Carey, F. G. *J. Biol. Chem.* **1977**, *252*, 4098.
(47) Alden, R. G.; Satterlee, J. D.; Mintorovitch, J.; Constantinidis, I.; Ondrias, M. R.; Swanson, B. I. *J. Biol. Chem.* **1989**, *264*, 1933.
(48) Benson, Jr., A. M.; Drickamer, H. G. *J. Chem. Phys.* **1957**, *27*, 1164.
(49) Wiederkehr, R. R.; Drickamer, H. G. *J. Chem. Phys.* **1958**, *28*, 311.
(50) Buckingham, A. D. *Proc. R. Soc. A* **1958**, *248*, 169.

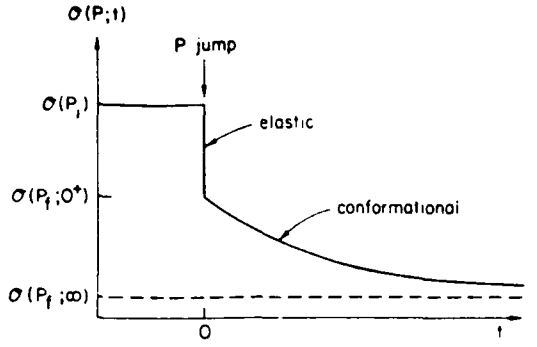

Figure 12. The behavior of an observable $O(P;t)$ after a rapid pressure change at time $t = 0$. An essentially instantaneous elastic relaxation is followed by a slower conformational relaxation.

Pressure is also a good tool with which to explore the dynamics of proteins.

7.1. The Pressure Jump Technique.[51] In the transition region shown in Figure 8 between about 150 and 210 K, the relaxation phenomena are slow enough to permit the determination of the relaxation functions with a Fourier-transform infrared spectrometer.[21]

The idea of a pressure jump experiment is simple. Consider an observable $O(P,T;t)$ that depends on pressure, with an equilibrium value $O(P,T;\infty) \equiv O(P,T)$. The system is first equilibrated at a given temperature T with pressure P_i. At time $t = 0$, the pressure is changed rapidly to a new value P_f and the change of the observable $O(P,T;t)$ as a function of time after the pressure change is measured. The general behavior of $O(P,T;t)$ after such a pressure jump is shown schematically in Figure 12. Initially $O(P,T;t)$ changes very rapidly from $O(P_i,T)$ to a value $O(P_f,T;0^+)$. We identify this change as *elastic relaxation*.[36] In a second phase, $O(P,T;t)$ relaxes with measurable rate toward the new equilibrium value $O(P_f,T;\infty)$. We interpret the second change as the *conformational relaxation* and characterize it at the temperature T by the relaxation function $\Phi(T;t)$,

$$\Phi(T;t) = \frac{O(P_f,T;t) - O(P_f,T;\infty)}{O(P_f,T;0^+) - O(P_f,T;\infty)} \qquad (18)$$

The experimental determination of $\Phi(T;t)$ is made difficult by the nonexponential character of the conformational relaxation. After the pressure jump, the experiment must be continued long enough so that the final value $O(P_f,T;\infty)$ is sufficiently well-known.

7.2. Time and Temperature Dependence of Φ. The relaxation functions observed in complex systems are usually not exponential in time and cannot be characterized by a single rate coefficient.[52-54] It is customary to approximate their time dependence either by a stretched exponential

$$\Phi(T;t) = \exp[-(k_r(T)t)^{\beta}] \qquad (19)$$

or by a power law[14]

$$\Phi(T;t) = [1 + k_r(T)t]^{-n} \qquad (20)$$

The parameters k_r, β, and n in eq 19 and 20 are usually functions of T. The rate parameter $k_r(T)$ follows an Arrhenius relation only over small intervals in T. In glasses, $k_r(T)$ can be described over more than 10 orders of magnitude either by the Vogel-Tammann-Fulcher equation[55]

$$k_r(T) = A_V \exp[-E_V/R(T-T_V)] \qquad (21)$$

or by the relation[56,57]

$$k_r(T) = A_B \exp[-(E_B/RT)^2] \qquad (22)$$

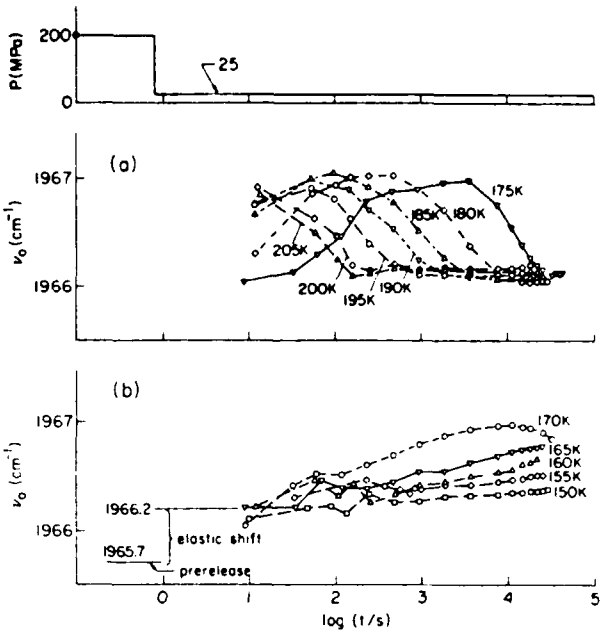

Figure 13. The peak wavenumber $\nu_0(t)$ of the A_0 band plotted versus log t in a pressure-release experiment. Top: Pressure plotted versus log t. Bottom: (b) 150–170 K. The elastic shift (0.5 cm^{-1}) is shown together with the prerelease wavenumber. (a) 175–205 K. Sample: swMbCO in 75% glycerol/water at pH 6.6.

Equation 22 contains only two free parameters and consequently yields better determined parameters than eq 21 if data are available only over small temperature intervals.

7.3. Relaxation Processes in swMbCO. The results presented in Figures 6 and 9 provide us with three observables $O(P;t)$ for studying the relaxation processes in MbCO: the relative areas, the peak wavenumbers, and the widths of the CO stretch bands A_i. The information in section 2 permits a logical connection between these observables and the tiers of substates. The three CO stretch bands label the three substates of tier 0. Exchange between these CS^0 after a perturbation, for instance a pressure jump, hence characterizes FIM 0, the nonequilibrium motion among CS^0. The peak wavenumber and width of an individual CO stretch band characterizes the substates of tier 1 within a given CS^0. We therefore assume that, in the absence of exchange with another CS^0, the motions of these observables after a perturbation label FIM 1, the nonequilibrium motion among the CS^1 of a given CS^0.

We have already published a set of relaxation data obtained with the pressure-release technique.[21] These experiments were performed with swMbCO in 75% glycerol/water (v/v) at pH ≈ 7 by applying 100 MPa at 240 K, cooling the sample to the desired temperature in the transition region between 160 and 205 K, measuring the IR spectrum for about 300 s, and releasing the pressure to 7 MPa in a few seconds. IR spectra were then taken at approximately exponentially increasing times from 10 to more than 10^4 s. The relaxation functions $\Phi_0(t)$ and $\Phi_1(t)$ were determined by eq 18 where O is the area of band A_0 for Φ_0, and the peak wavenumber or width of A_0 for Φ_1. The resulting relaxation functions are shown in ref 21 and reveal two characteristics that are also seen in relaxation processes in glasses: The relaxation functions are nonexponential in time, and the relaxation rates differ by orders of magnitude in a narrow temperature interval suggesting a non-Arrhenius temperature behavior. The time dependence of $\Phi_1(t)$ was fit by using a power law, eq 20, which describes the data better than a stretched exponential, eq 19.

A new set of pressure release data on MbCO in 75% glycerol/water at pH 5.5 and 6.6 again shows the two relaxation processes FIM 0 and FIM 1 but surprisingly also gives evidence for a third relaxation process near 180 K. The data were taken by

(51) Attwood, P. V.; Gutfreund, H. *FEBS Lett.* **1980**, *119*, 323.
(52) Wagner, K. W. *Ann. Phys.* **1913**, *40*, 817.
(53) Klafter, J.; Shlesinger, M. F. *Proc. Natl. Acad. Sci. USA* **1986**, *83*, 848.
(54) Shlesinger, M. *Annu. Rev. Phys. Chem.* **1988**, *39*, 269.
(55) Zallen, R. *The Physics of Amorphous Solids*; Wiley: New York, 1983. Jäckle, J. *Rep. Prog. Phys.* **1986**, *49*, 171.
(56) Bässler, H. *Phys. Rev. Lett.* **1987**, *58*, 767.
(57) Zwanzig, R. *Proc. Natl. Acad. Sci. USA* **1988**, *85*, 2029.

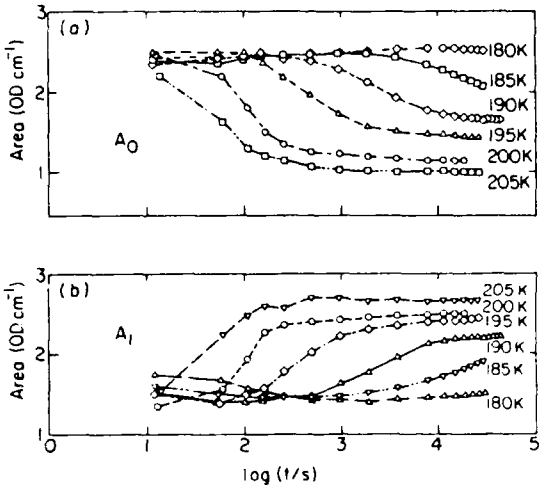

Figure 14. The areas of the bands A_0 and A_1 as a function of time after a pressure release from 200 to 25 MPa. Temperature, 180–205 K. Sample: swMbCO in 75% glycerol/water at pH 6.6.

applying 200 MPa at 225 K, cooling the sample to the desired temperature, measuring the IR spectrum for about 300 s, and releasing the pressure to 25 MPa in a few seconds. Infrared spectra were again taken at approximately exponentially increasing times from about 10 to 10^4 s. Figure 13 shows the peak wavenumber ν_0 for band A_0 at pH 6.6 from 150 to 205 K plotted versus log t. Figure 14 shows the areas of A_0 and A_1 as a function of time after pressure release. The data in these figures suggest the following sequence of relaxations in the transition region near T_{sg}:

$$1965.7 \xrightarrow{\text{elastic}} 1966.2 \xrightarrow{\text{FIM 1}} 1967.0 \xrightarrow{\text{FIM X}} 1966.2 \xrightarrow{\text{FIM 0}} 1966.2\ \text{cm}^{-1}$$

After the pressure release, a rapid elastic shift changes the peak position of A_0 from 1965.7 to about 1966.2 cm^{-1}. Below about 150 K, no further shift occurs. Above about 150 K, the peak position of A_0 does not stop at 1966.2 cm^{-1} but continues to shift to the blue with a nonexponential time dependence. Above 180 K, FIM 1 is so fast that relaxation appears to start at 1967.0 cm^{-1}. Surprisingly, however 1967.0 cm^{-1} does not correspond to the relaxed pressure state F, 1966.2 cm^{-1}. Indeed, a new relaxation process occurs which leads from 1967.0 to 1966.2 cm^{-1}. Since we do not yet have a satisfactory interpretation of this relaxation process, we call it FIM X. Above 180 K, FIM 0 sets in; it is the transition from substate A_0 to A_1 measured by the change in area of A. Above about 210 K, FIM 0 becomes too fast to be observed with our system.

In addition to the three relaxation processes FIM 0, 1, and X at least one other similar process occurs near 180 K: the exchange between the substates A_1 and A_3.[21] We have not yet investigated this exchange in detail; its study will require pH greater than 7.

To evaluate the relaxation data, we first calculate the relaxation functions $\Phi(t)$, eq 18. The observable O in eq 18 is the peak frequency or width of A_0 for FIM 1, the peak frequency of A_0 for FIM X, and the area of A_0 for FIM 0. The three relaxation functions, displayed in Figure 15, show that FIM 1 and FIM 0 are clearly nonexponential in time, while FIM X is close to an exponential. A stretched exponential, eq 19, fits FIM 1 better than a power law, eq 20, at pH 5.5 and 6.6. Previously, FIM 1 was fit to a power law at pH 7.[21] Because the deconvolution of the infrared spectra into A_0, A_1, and A_3 is somewhat ambiguous, the details of the time dependence are difficult to pin down. To further evaluate the data, we fit the temperature dependence of the relaxation functions in two different ways, with an Arrhenius relation and with eq 22. The results, together with the values from ref 21, are given in Table IV.

Even though the data in Table IV are preliminary, they provide insight into the relaxation processes in Mb. We first note that FIM X differs considerably from FIM 0 and FIM 1. Its preexponential factor as obtained from an Arrhenius relation is close to the normally expected value of 10^{12} s^{-1}, and the activation energy could place it into tier 2. Moreover, it is close to exponential in time. We therefore believe that it describes a less complex phenomenon than either FIM 0 or FIM 1. In earlier experiments[21] at a higher pH we did not observe FIM X; it may consequently be strongly influenced by pH. The curves in Figure 13 hint that more detailed studies of FIM X and of the state with wavenumber 1967.0 cm^{-1} are feasible: Near 180 K, Mb remains in this state

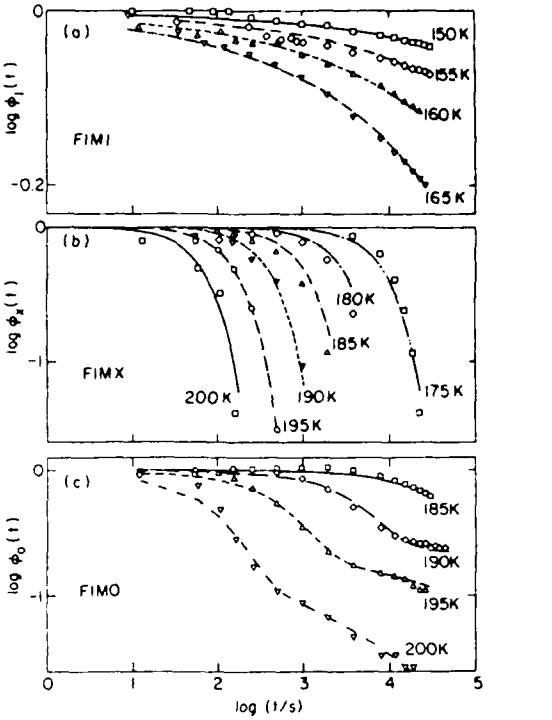

Figure 15. Relaxation functions $\Phi(t,T)$, eq 18, for FIM 1, FIM X, and FIM 0. FIM 1 was obtained by using the decrease in width of A_0. FIM X is characterized by the shift of the peak wavenumber of A_0. FIM 0 is characterized by the change in the area of A_0. Sample: swMbCO in 75% glycerol/water at pH 6.6.

TABLE IV: Parameters Characterizing the Relaxation Processes FIM 0, FIM 1, and FIM X[a]

parameter	pH	FIM 0 fast	FIM 0 slow	FIM 1	FIM X
		Time Dependence			
β	5.5	*b*	*b*	0.3	≈1
	6.6	≈1	0.2	0.3	≈1
	≈7	≈1	0.8	*c*	
		Temperature Dependence–Arrhenius, $k = A \exp(-E/RT)$			
log (A/s^{-1})	5.5	*b*	*b*	20	12
	6.6	27	70	20	13
	≈7			36	
E, kJ/mol	5.5	*b*	*b*	75	55
	6.6	110	280	80	55
	≈7			125	
		Temperature Dependence, $k = A_B \exp(-(E_B/RT)^2)$, Eq 22			
log (A_B/s^{-1})	5.5	*b*	*b*	8	5
	6.6	13	34	7	5
	≈7	13	21	17	
E_B, kJ/mol	5.5	*b*	*b*	7	6
	6.6	9	15	7	7
	≈7	10	13	9	

[a] The time dependence of the relaxation function $\Phi(t,T)$ described by a stretched exponential, eq 19, with parameter β. Temperature dependence given in terms of an Arrhenius (A,E) and eq 22 (A_B,E_B). FIM 0 has a fast and slow component for pH 6.6 and ≈7.[21] FIM X is not observed for pH ≈ 7. Errors are ±25%. [b] Parameters not well determined. [c] FIM 1 for pH ≈ 7 is better described by a power law, eq 20 with n = 0.26.

for a sufficiently long time so that additional measurements can be performed.

FIM 0 and FIM 1 are both nonexponential in time. FIM 1 can be well described by a stretched exponential. FIM 0, on the other hand, is more complicated. The data in Figures 14 and 15 and at higher pH[21] suggest a biphasic behavior in which at least one or, possibly, both of the components display a nonexponential time dependence. We cannot yet decide if the relaxation is due to one rather complex process or if two different phenomena are involved. Moreover, interference from FIM X is possible. To obtain some insight, we fit Φ_0 with two components where one is a stretched exponential while the other is close to exponential. These components are labeled "slow" and "fast" in Table IV. The temperature dependencies of FIM 0 and FIM 1 are not adequately described by an Arrhenius relation, because the preexponentials take on values of 10^{20} s^{-1} and higher. Similar values of the preexponentials arise if the α relaxation in glasses is characterized by an Arrhenius relation. In glasses, where the α relaxation can be observed over a wide range in T, it is known that an Arrhenius plot does not yield a straight line and that, for instance, eq 21 or 22 must be used. We invoke the analogy to glasses and use eq 22 to parametrize the data in Table IV. The values of the preexponential and energy for FIM 1 appear to depend strongly on pH. We assume, again in analogy to glasses, that both FIM 0 and FIM 1 describe large-scale motions in the protein. A complete characterization of relaxation in MbCO is difficult owing to the fact that several relaxation processes occur in a narrow temperature interval around 180 K. In addition, the biphasic nature of FIM 0 is not understood. Therefore, all relaxation processes in MbCO will have to be studied in more detail before they can be fully interpreted.

8. Pressure and Protein Reactions

We discuss here one simple example, the binding of CO and O_2 to myoglobins at low temperatures, but believe that the general concepts will be needed to explain the high-temperature data and are also applicable to other reactions in complex systems.

8.1. Pressure Effect on Ligand Binding—A Puzzle? The measurements of the effects of pressure on the association rates of CO and O_2 to Mb and hemoglobin (Hb) by Hasinoff[58] gave a puzzling result. The activation volumes [eq 4] for the binding of O_2 were positive (+8 cm^3/mol for Mb, +5 cm^3/mol for Hb) while those for CO were negative (−9 cm^3/mol for Mb, −3 and −21 cm^3/mol for the "fast" and "slow" reaction in Hb). The negative values observed for CO conform to expectation: The binding of CO involves formation of a covalent bond between CO and the heme iron, and such bond formation is typically characterized by an activation volume of about −10 cm^3/mol.[59] In contrast, the positive activation volume for O_2 is surprising. The puzzle is magnified on closer inspection. The binding of CO and O_2 is controlled at the heme iron, and this binding step is similar for both ligands.[60] Moreover, binding of CO to heme has an activation volume of +2 cm^3/mol.[61] These values demonstrate that the binding process is more complex than a simple one-step reaction and that the protein must play a role in the control of the binding reaction. We will show here that the effect of pressure on the simple association reaction is sufficiently complex that experiments performed only at physiological temperatures and using only observation in the Soret are incapable of elucidating the mechanisms of such biomolecular reactions.

8.2. Low-Temperature Binding of CO and O_2 to Mb. In order to discuss the effect of pressure on the binding of ligands to heme proteins, the general features of the binding process must be described first. While pressure data over the entire temperature range from 4 to 300 K exist,[62] we restrict the discussion here to the low-temperature regime below about 160 K. This restriction

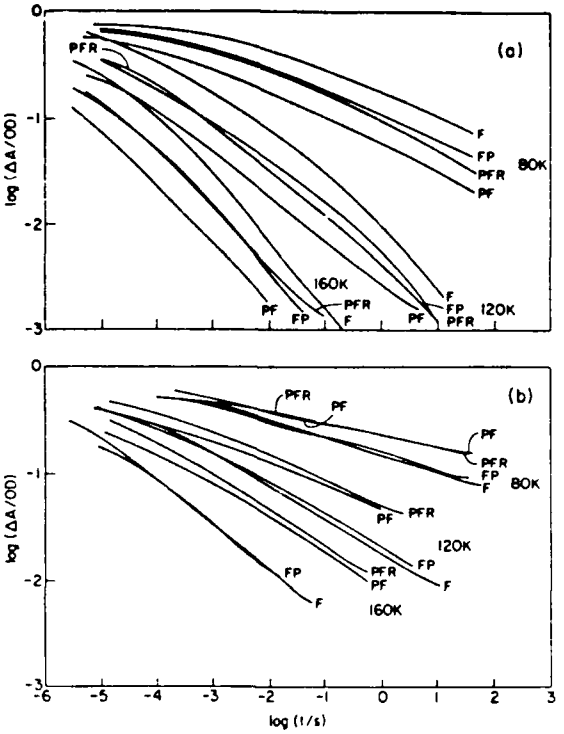

Figure 16. Rebinding of CO (a) and O_2 (b) to sperm whale myoglobin after flash photolysis. $\Delta A(t)$, the absorption change at time t after the laser flash, is proportional to the fraction of Mb molecules that have not rebound a ligand. The data have been scaled to $\Delta A(0)$ for swMbCO in the F state. Solvent: 75% glycerol/water, pH 7.0. The pressure states F, FP, PF, and PFR are defined in Figure 8.

permits us to concentrate on the central aspects of the binding reaction.

The binding of CO and O_2 to heme proteins at temperatures below about 160 K has been studied in detail by using flash photolysis.[14,63] The sample, for instance MbCO, is brought to the desired temperature. The bond between the CO and the heme iron is broken by a laser flash. The CO moves into the heme pocket and rebinds from there. We denote the bound state as A and the state with the ligand in the heme pocket by B (Figure 1b). Rebinding B → A is monitored by observing the corresponding spectral changes, either in the Soret[14] or the infrared.[11] We denote with $N(t)$ the survival probability, the fraction of Mb molecules that has not rebound a ligand at the time t after photodissociation. $N(t)$ is *nonexponential* in time and can usually be approximated by a power law, eq 20.[14] Examples of such nonexponential rebinding are given in Figures 16 and 17.

The nonexponential rebinding is explained by postulating that each protein molecule is in a different conformational substate and that the different substates possess different activation enthalpies H_{BA} for the binding transition B → A.[14] To describe the observed $N(t)$, we write

$$N(t) = \int dH_{BA}\, g(H_{BA}) \exp[-k(H_{BA})t] \qquad (23)$$

Here $g(H_{BA})\, dH_{BA}$ is the probability of finding a protein molecule with an enthalpy barrier between H_{BA} and $H_{BA} + dH_{BA}$, and $k(H_{BA})$ is the rate coefficient

$$k(H_{BA}) = A_{BA} \exp[-H_{BA}/RT] \qquad (24)$$

The preexponential, A_{BA}, is usually taken as $A_{BA} = A(T/T_0)$, where the reference temperature T_0 is 100 K and A is temperature independent.

8.3. Pressure Effects Observed in the Soret Band.[40] We expect pressure to have two dominant effects on reaction rates, similar

(58) Hasinoff, B. B. *Biochemistry* **1974**, *13*, 3111.
(59) Van Eldick, R.; Asano, T.; Le Noble, W. J. *Chem. Rev.* **1989**, *89*, 549.
(60) Frauenfelder, H.; Wolynes, P. *Science* **1985**, *229*, 337.
(61) Caldin, E. F.; Hasinoff, B. B. *J. Chem. Soc., Faraday Trans. 1* **1975**, *71*, 515.
(62) Alberding, N. A. Ph.D. Thesis, University of Illinois at Urbana-Champaign, 1978.
(63) Ansari, A.; Di Iorio, E. E.; Dlott, D. D.; Frauenfelder, H.; Iben, I. E. T.; Langer, P.; Roder, H.; Sauke, T. B.; Shyamsunder, E. *Biochemistry* **1986**, *25*, 3139.

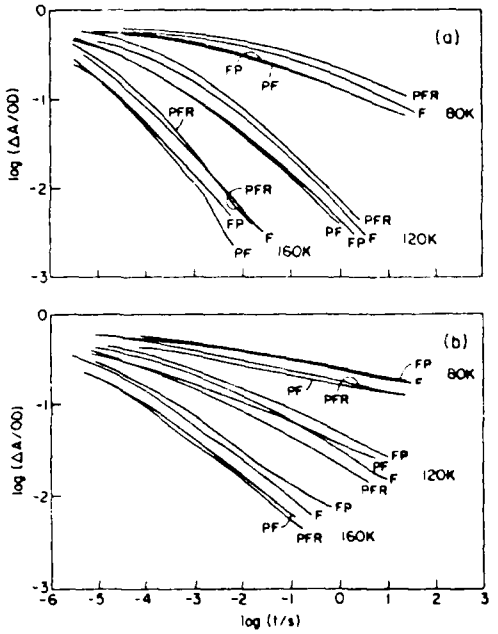

Figure 17. Rebinding of CO (a) and O_2 (b) to horse myoglobin after photodissociation. The data have been scaled to $\Delta A(0)$ for swMbCO in the F state. Solvent 75% glycerol/water, pH 7.0.

to the two effects on spectral line shifts. In each given conformational substate, the reaction rate will be changed through the activation volume according to eq 3 and 4. Pressure can, however, also shift the populations among substates and thus affect the reaction rate. To separate the two phenomena, we use the technique shown in Figure 8 and described in section 6 for spectral shifts.

The pressure experiment is, in principle, straightforward. We observe rebinding after flash photolysis for the four pressure states F, FP, PF, and PFR of Figure 8 for sperm whale (swMb) and horse (hMb) myoglobin. In practice, low-temperature high-pressure flash photolysis experiments lead to many experimental frustrations, and the help and guidance of Harry Drickamer has been essential for this work. A selection of experimental results are shown in Figure 16 and 17, where log $\Delta A(t)$ is plotted versus log t. The absorbance change $\Delta A(t)$ at time t is proportional to the survival probability $N(t)$, eq 23. The binding of CO was monitored at 436 nm and that of O_2 at 440 nm.

Even without detailed evaluation, the data in Figures 16 and 17 show that both activation and conformation effects are present, that sperm whale and horse Mb behave differently, and that CO and O_2 also display clear differences.

8.4. Evaluation of the Pressure Data. Evaluation entails three aspects: the nonexponential time dependence, extraction of activation volumes, and interpretation.

The nonexponential time dependence is described in terms of the probability density $g(H_{BA})$ in eq 23. In principle, we can invert eq 23 for each pressure state and find the distributions for the four pressure states.[40] However, this procedure does not yield activation volumes directly and is technically often difficult because $N(t)$ cannot easily be measured over a sufficiently extended time range. We introduce here a simple approach that gives some of the essential information directly. Consider the nonexponential rebinding curve and the corresponding probability density distribution shown in Figure 18. Equation 23 shows that at a given time τ only a small band of activation enthalpies contributes to the rebinding. Proteins with rates satisfying $k(H_{BA})\tau \gg 1$ have already rebound their ligand while those with $k(H_{BA})\tau \ll 1$ rebind much later. Only proteins with barriers centered at

$$H_{BA}(\tau) = RT \ln [A_{BA}\tau] \qquad (25)$$

contribute to binding at time τ. We use a temperature-independent preexponential A_{BA} in eq 25 for simplicity. Equation 25 assigns

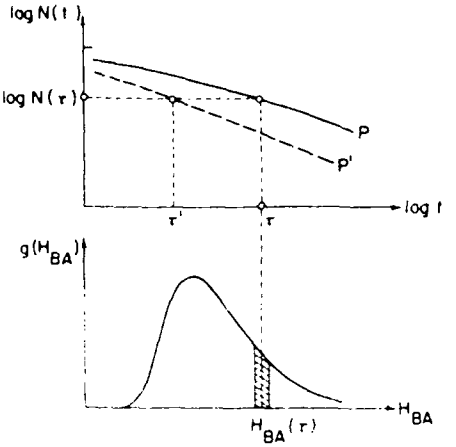

Figure 18. Nonexponential rebinding, $N(t)$, and the corresponding probability density distribution, $g(H_{BA})$. At the time τ only proteins with enthalpies near $H_{BA}(\tau)$ rebind.

an average activation enthalpy $H_{BA}(\tau)$ to each time τ.

This approach permits us to find an approximate value for the activation volume: Pressure, as indicated in Figure 18, can change the rebinding. If no conformational changes occur, the shift from τ to τ' at constant $N(\tau)$ is caused by an *activation volume*. The pressure dependence of the rate coefficient is given by eq 3 and 4 as $k(P) = \text{const} \times \exp[-PV^*_{BA}/RT]$. If $k(P)$ is measured at two pressures, P and P', the activation volume is obtained from the ratio $k(P)/k(P')$ as

$$V^*_{BA} = \frac{RT}{P' - P}\{\ln k(P) - \ln k(P')\} \qquad (26)$$

With $k(P) = 1/\tau(P)$, eq 26 permits the immediate evaluation of the activation volume from the data in Figures 16 and 17. Moreover, by obtaining V^*_{BA} at various values of $N(\tau)$, we find the dependence of the activation volume on the barrier enthalpy at the initial pressure. Since the barrier enthalpy characterizes the substates, we are able to investigate the substate dependence of V^*_{BA}.

If pressure causes a conformational change, the situation is different. The two curves labeled P and P' in Figure 18 then can correspond to the same external pressure, but to different conformations. The curves labeled F and PFR in Figures 16 and 17 represent such a pair. We can, nevertheless, use eq 26 to define a *conformation volume* V_C to describe the rate change in going at a fixed value of $N(\tau)$ from τ to τ'. The pressures P and P' then do not correspond to the external pressure, but to the pressures at which the sample was frozen. Rebinding data taken at the four points F, FP, PF, and PFR in the PT plane (Figure 8) thus permit the definition of three activation volumes

$$V^*_1 \equiv V_{FP\text{-}F}, \quad V^*_2 \equiv V_{PF\text{-}PFR}, \quad V_C \equiv V_{PFR\text{-}F} \qquad (27)$$

The subscripts indicate between which pairs of curves the difference $\{\ln k(P) - \ln k(P')\}$ has to be taken. The pressure difference for all volumes is the pressure at the points 0 and P in Figure 8. V^*_1 and V^*_2 are activation volumes. V_C, the conformation volume, is a parameter with units of volume, but with no direct interpretation in terms of a real volume. V_C expresses the direction and effect of conformational changes.

Values of the activation and conformation volumes, obtained with eq 26 from the data in Figures 16 and 17, are given in Table V. $N(\tau)$ is defined in Figure 18. $H_{BA}(\tau)$ is obtained from eq 25, with temperature-independent preexponentials obtained by using a gamma distribution for $g(H_{BA})$.[64]

The values in Table V show that horse and sperm whale myoglobin behave very differently under pressure even though the rebinding curves at $P = 0$ look very similar. In both proteins, the activation volumes for MbCO are negative and of the expected

(64) Young, R. D., Bowne, S. F. *J. Chem. Phys.* **1984**, *81*, 3730.

TABLE V: Activation Volumes $V^{\ddagger}_1$ and $V^{\ddagger}_2$ and Conformation Volume V_C Describing the Effect of Pressure on the Four States of Figure 8[a]

sample	T, K	$\Delta A(\tau)$ (OD)	$H_{BA}(\tau)$, kJ/mol (state F)	$V^{\ddagger}_1$, cm³/mol	$V^{\ddagger}_2$, cm³/mol	V_C, cm³/mol
swMbCO	80	0.3	12	−8	−7	−8
		0.1	16	−7	−7	−9
	120	0.1	16	−9	−7	−9
		0.01	21	−6	−7	−9
$swMbO_2$	80	0.3	12	−2	0	+7
	120	0.3	12	−2	−7	+7
		0.1	16	0	−3	+13
hMbCO	80	0.3	13	−5	−10	+4
	120	0.3	12	−6	−10	+5
		0.1	16	−5	−8	+3
		0.01	21	−3	−6	+2
$hMbO_2$	80	0.3	13	0	−4	−8
	120	0.3	13	+2	−1	−7
		0.1	18	+4	+4	−7

[a] Temperature-independent preexponentials, A_{BA}: 1.2×10^9 s^{-1} (swMbCO), 1.8×10^9 s^{-1} ($swMbO_2$), 2.0×10^9 s^{-1} (hMbCO), 1.8×10^9 s^{-1} ($hMbO_2$). Rebinding monitored in Soret band; MbCO at 436 nm, MbO_2 at 440 nm. Samples: sperm whale (swMb) and horse (hMb) myoglobin in 75% glycerol/water (v/v) with phosphate buffer, pH 7.0. Error in V is ±1 cm³/mol.

TABLE VI: Activation and Conformation Volumes of the Substates A_0 and A_1 for Binding of CO to Sperm Whale Myoglobin[a]

substate	pH	T, K	$N(\tau)$	$H_{BA}(\tau)$, kJ/mol (state F)	$V^{\ddagger}_1$, cm³/mol	$V^{\ddagger}_2$, cm³/mol	$V^{\ddagger}_C$, cm³/mol
sum	5.5	25	0.5	7	−4		−16
A_0			0.6	7	0		−12
sum	6.6	40	0.5	11	−10	−2	−19
A_0			0.3	11	−5	−2	−11
A_1			0.6	10	−8	−2	−5
sum	6.6	50	0.3	13	−8	−3	−15
A_0			0.1	15	−4	−3	−11
A_1			0.3	13	−9	−5	−5

[a] Preexponentials for: A_0 and A_1 from ref 11. The 50 K data are not shown in the figures. Error in V is ±1 cm³/mol. Solvent: 75% glycerol/water (v/v) and potassium phosphate buffer.

magnitude for bond formation; pressure speeds up CO rebinding. The magnitude of the activation volume for CO decreases with increasing barrier height. The activation volume for rebinding of O_2 is small for both swMb and hMb, but clearly negative for swMb and mostly positive for hMb. These values for dioxygen solve part of the puzzle created by the room temperature measurements: The activation volume for the rebinding step at the heme is not large and positive, but small and mainly negative. The conformational effects, which are characterized by V_C, are large and negative for swMbCO and $hMbO_2$, large and positive for $swMbO_2$, and small and positive for hMbCO. The large difference between the conformation volumes for swMbCO (−9 cm³/mol) and $swMbO_2$ (+7 to +13 cm³/mol) obtained from the Soret band suggests a strong interplay between ligand and protein.

8.5. CO Rebinding Observed in the Infrared Spectrum. The Soret data show that protein structure and ligand properties affect the pressure dependence of ligand binding, but they cannot tell us which tier of substates is responsible. This information is obtained by monitoring the ligand rebinding using the infrared CO stretch bands. Rebinding data after flash photolysis for the bands A_0 and A_1 are given in Figures 19 and 20. At pH 6.6, both bands can be measured; at pH 5.5, the A_1 band in the states PF and PFR is too small to be measured. Figures 19 and 20 show that pressure affects the rebinding in both substates but that the changes differ considerably for the two bands. From the measured curves, the activation volumes $V^{\ddagger}_1$ and $V^{\ddagger}_2$ and the conformation volume V_C are determined by the method described in subsection 8.4; the results are summarized in Table VI. The data in Table VI and the curves in Figure 19 show that the speed-up of the CO rebinding has two causes: Pressure shifts the population from the

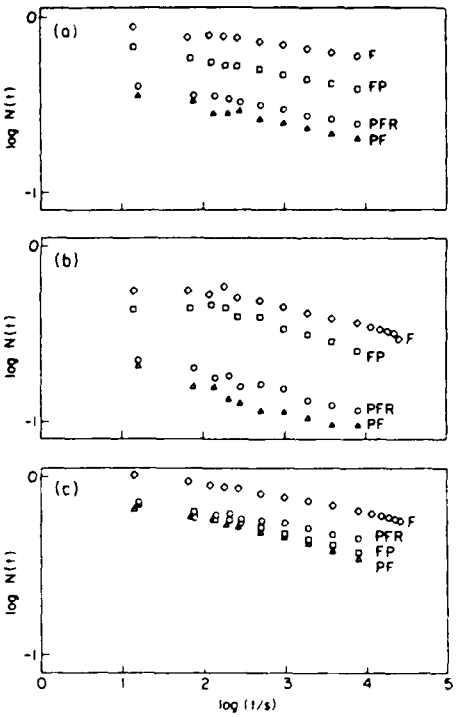

Figure 19. Rebinding of CO to swMb after photodissociation at 40 K as a function of time for different pathways (see Figure 8). (a) Rebinding of the total A substates; (b) rebinding to A_0; (c) rebinding to A_1. Sample: swMbCO in 75% glycerol/water (v/v) at pH 6.6.

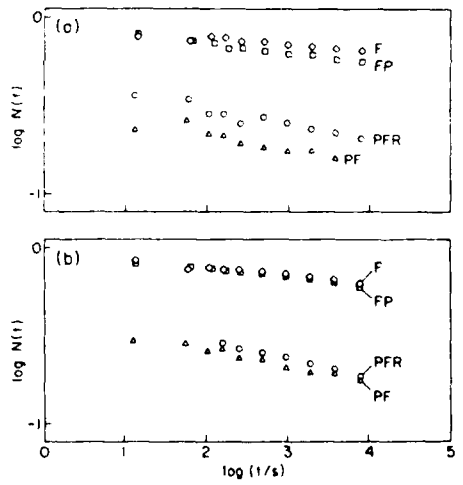

Figure 20. Rebinding of CO to swMb after photodissociation at 25 K as a function of time for different pathways (see Figure 8). (a) Rebinding of the total A substates; (b) rebinding to A_0. Sample: swMbCO in 75% glycerol/water (v/v) at pH 5.5.

slower A_1 substate to the faster A_0 substate, and the rebinding of both substates speeds up. The rebinding of each substate is nonexponential in time. These results require a generalization of eq 23 to include multiple A substates:

$$N(t) = \sum_i w_i(P) \int dH_{BA}\, g_i(H_{BA}) \exp[-k_i(H_{BA})t] \quad (28)$$

The sum extends over the substates of tier 0, $w_i(P)$ is the weight of substate A_i at pressure P, and $g_i(H_{BA})$ is the corresponding probability distribution of the barrier height. The rate coefficients $k_i(H_{BA})$ are given by eq 24, but the preexponential A_{BA} may be different for each substate.[11] The speed up for CO rebinding to swMB is described by the changes in the weights $w_i(P)$ and in the distributions $g_i(H_{BA})$.

The two substates A_0 and A_1 behave differently under pressure as indicated by the parameters in Table VI. The increased re-

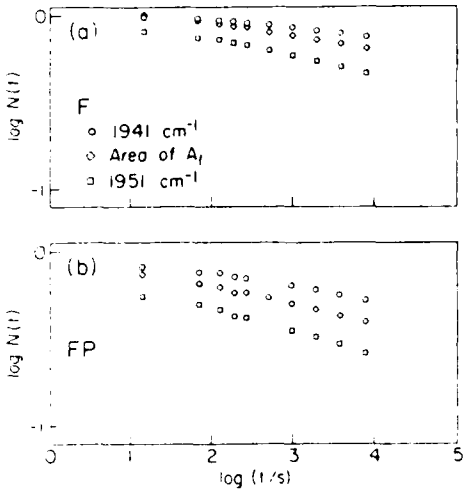

Figure 21. Rebinding of CO to swMb after photodissociation at 40 K as a function of time at different wavenumbers. (a) State F; (b) state FP. Sample: swMbCO in 75% glycerol/water (v/v) at pH 6.6. (○) 1941 cm^{-1}, (◇) area of A_1, (□) 1951 cm^{-1}.

binding rate of A_0 is caused by a large conformation volume, while the increase in A_1 is the result of a large activation volume. Pressure thus mainly affects $g_0(H_{BA})$ and $k_1(H_{BA})$. The difference between A_0 and A_1 is also evident when the rebinding is monitored at different wavenumbers within the same A band. Each substate of tier 0 is comprised of a large number of substates of tier 1 and is inhomogeneously broadened. If these CS^1 have different activation energies, different wavenumbers within the same band should rebind differently at $P = 0$ (state F). This effect is called kinetic hole burning.[16,17,19] Figure 21a shows that this prediction is indeed true for A_1. If different CS^1 also have different activation volumes, rebinding in the state FP should differ from that in F. Figure 21b shows that the rate increase from 1941 to 1951 cm^{-1} is indeed larger in FP than in F. In substate A_1, both activation and conformation effects are important. In contrast, kinetic hole burning is very small in A_0.

In Table VI, the activation and conformation volumes are listed for the sum of the A substates. We would expect the sum of the infrared bands to give the same parameters as the Soret band. While the two sets show the same trend, there are quantitative differences. V^*_2, in particular, is much smaller in the infrared than in the Soret band. The different measurement techniques may be responsible for the discrepancy: In the IR regions the band areas are monitored; in the Soret region, only a small wavelength band is observed. The discrepancy thus leads to a prediction, not yet tested: The pressure effect observed should depend on wavelength in the Soret region, just as in the IR region.

The MbCO results obtained in the infrared region permit some indirect conclusions about the binding of dioxygen. The stretch bands of O_2 are difficult to observe and make the IR monitoring of O_2 binding nearly impossible. However, the data in Table V show that V_C for O_2 binding to swMb is large and positive: Pressure slows down O_2 binding and the main cause for the slowdown is a conformational shift and not an activation volume. In contrast, the binding of O_2 to horse myoglobin is more weakly affected by pressure, and the conformation volume has the opposite sign from swMb. It is amusing to speculate whether the difference is related to the fact that whales dive and horses do not.

8.6. A Model of Activation and Conformation Effects. The evaluation introduced in subsection 8.4 is only semiquantitative. A full treatment of the data is very complicated, and we will not perform it here. We will, however, sketch the approach for the simple situation shown in Figure 1. We assume two conformational substates of tier 0, labeled 0 and 1. The protein then has four states, the bound substate A_0 and A_1 and the two photodissociated pocket states B_0 and B_1. The notation for the B_0 substate differs from previous usage.[11] Two conformational transitions, $A_0 \leftrightarrow A_1$ and $B_0 \leftrightarrow B_1$, and two reactions, $B_0 \rightarrow A_0$ and $B_1 \rightarrow A_1$, can occur.[65] At high temperatures, the two types of transitions may have about equal rates. Here we discuss low temperatures, $T < T_{sg}$, where conformational transitions are absent, as was discussed in sections 5 and 7. The survival probability $N(t)$ of the photodissociated species can then be written as

$$N(t) = w_0(P) \exp\{-k_0(P)t\} + w_1(P) \exp\{-k_1(P)t\} \quad (29)$$

Here $w_0(P)$ and $w_1(P)$ are the substate populations, and $k_0(P)$ and $k_1(P)$ are the rate coefficients for CO binding from substates B_0 and B_1. The survival probabilities $N(\tau)$ at time τ (Figure 18) for the four pressure states of Figure 8 are

$$N_F(\tau) = w_0(0) \exp\{-k_0(0)\tau\} + w_1(0) \exp\{-k_1(0)\tau\}$$

$$N_{FP}(\tau) = w_0(0) \exp\{-k_0(P)\tau\} + w_1(0) \exp\{-k_1(P)\tau\}$$

$$N_{PF}(\tau) = w_0(P) \exp\{-k_0(P)\tau\} + w_1(P) \exp\{-k_1(P)\tau\}$$

$$N_{PFR}(\tau) = w_0(P) \exp\{-k_0(0)\tau\} + w_1(P) \exp\{-k_1(0)\tau\} \quad (30)$$

Following the arguments in section 6.1, we introduce three independent differences. With the normalization $w_0(P) + w_1(P) = 1$, and the abbreviations

$$\delta_i(\tau) = \exp[-k_i(P)\tau] - \exp[-k_i(0)\tau], \quad i = 0, 1 \quad (31)$$

we obtain

$$\Delta_1'(\tau) = N_{FP}(\tau) - N_F(\tau) = w_0(0)\,\delta_0(\tau) + w_1(0)\,\delta_1(\tau)$$

$$\Delta_2'(\tau) = N_{PF}(\tau) - N_{PFR}(\tau) = w_0(P)\,\delta_0(\tau) + w_1(P)\,\delta_1(\tau)$$

$$\Delta_3'(\tau) = N_{PFR}(\tau) - N_F(\tau) = [w_1(P) - w_1(0)][\exp\{-k_1(0)\tau\} - \exp\{-k_0(0)\tau\}] \quad (32)$$

As in eq 14, we also form the difference

$$\Delta_2'(\tau) - \Delta_1'(\tau) = [w_1(P) - w_1(0)][\delta_1(\tau) - \delta_0(\tau)] \quad (33)$$

Similar arguments to those in section 6.1 show the following: nonvanishing Δ_1' and Δ_2' prove that the activation volumes for the substates are nonzero, nonvanishing Δ_3' shows that pressure changes the population of the substates and that the rates in the two substates are different; and a nonvanishing difference $\Delta_2' - \Delta_1'$ proves that the activation volumes affect $\delta_i(\tau)$ for the two substates differently.

While the approach given so far describes some of the main features of the observed pressure effects, it must be generalized in at least two ways: eq 29 assumes that rebinding is exponential in time for each substate. To take the nonexponential rebinding into account, eq 28 must be used. The second generalization is demanded by the hierarchy of substates. In eq 30, the same rate coefficients $k_0(P)$ and $k_1(P)$ are used for the two pressure states, FP and PF. The transitions $B_0 \rightarrow A_0$ and $B_1 \rightarrow A_1$ involve, however, a large number of transitions between substates of tier 1. Pressure changes the distribution of these CS^1, and the rates for each pressure state (FP, PF, F, and PFR) can be different. This difference is evident in Table VI where the parameters V^*_1 and V^*_2 are not identical. These generalizations exceed the scope of the present paper, and we consequently do not complete the evaluation here.

9. Summary and Outlook

As a thermodynamic variable, pressure is as important as temperature in the study of proteins. In the present paper, we have treated five areas where pressure is an essential tool (section 1). In each of the five areas, the pressure experiments have yielded new insights and opened new avenues. Pressure affects proteins differently than it does crystals because proteins are complex systems and can assume a large number of different conformational substates, arranged in a hierarchy of tiers (section 2). Pressure consequently affects proteins in two ways; it can act on a protein in a given substate (elastic effect), and it can shift the distribution of substates, thereby influencing protein structure, dynamics, and function (conformational effects).

(65) Frauenfelder, H.; Steinbach, P. J.; Young, R. D. *Chem. Scr.*, in press.

Myoglobin shows a glass transition near 180 K if embedded in a glycerol/water solvent. Well above the transition temperature, protein substates are in equilibrium and the thermodynamic parameters describing substates of tier 0, in particular their volume differences, can be determined (section 4). Our results imply that the internal energy, the entropy, and the volume of myoglobin are functions of temperature. The experiments also show that infrared measurements over a wide range in temperature are essential for protein studies; if data are taken only in the visible region or over a small temperature range, an unambiguous interpretation is difficult or impossible.

Below about 180 K, myoglobin becomes glasslike; the metastability is proven by combining pressure and temperature variations and demonstrating that the infrared spectrum of myoglobin depends on the path in the *TP* plane by which a final temperature–pressure point is reached (section 5).

The technique of taking different pathways to a given *TP* point below the glass temperature also permits the separation of elastic and conformational pressure effects on spectral bands (section 6). These experiments show that different substates of tier 0 possess different elastic and conformational properties.

One of the goals of protein studies is the measurement and description of protein motions. The pressure jump technique provides a generally applicable approach to explore protein motions (section 7); it shows that relaxation phenomena are complicated but can be unravelled.

The most important use of pressure may well be for the study of protein reactions. Here again the different pathways in the *PT* plane permit the separation of the effects of pressure into an activation and a conformation component, characterized by activation and conformation volumes (section 8). A surprising result of these studies is the large difference in behavior between closely related proteins such as sperm whale and horse myoglobin. While it is dangerous to extrapolate from a small sample, it appears that the pressure parameters give as much or more information than activation enthalpies.

The experiments and models treated in the present paper are only a beginning and call for a large number of additional experiments and for better theoretical treatments. Foremost is the extension of the experiments to other proteins, both wild-type and synthetic mutants. Without a larger data base the results cannot be fully interpreted. It is not clear which phenomena are general and which ones are specific (or accidental) in a particular protein. Equally important is the connection of the pressure data to structural and calorimetric measurements. The experiments described here show that the dynamic properties of myoglobin depend strongly on pH and suggest that even the overall structure and the specific heat may differ in the different substates of tier 0. X-ray and specific heat data as a function of pH can verify or discredit this model.

An ordinary glass usually shows one glass transition (α relaxation) with non-Arrhenius temperature dependence; secondary glass transitions (β,γ) are less pronounced.[55] Myoglobin shows at least three relaxation phenomena near 180 K. Two have properties characteristic of a glass transition, and the other may be similar to the β relaxation. Such a behavior is not entirely unexpected: Different domains[66] in the protein could well have related but somewhat different relaxation phenomena. The technique discussed in section 7 will permit more studies of these relaxation processes by looking not only at the CO stretch bands, but also at other IR bands.

The sensitivity of the rebinding to swMb and hMb to the activation and conformation volumes suggests another class of experiments. Monitoring rebinding in the IR and the use of different isotopes of C and O earlier permitted us to conclude that CO does not bind like a point particle, but must undergo some rotational motion.[67] The combination of isotopic replacements with rebinding measurements at various points in the *TP* plane should provide an even closer look at the binding step at the heme iron.

In the present paper we discussed only the binding of CO and O_2 below 180 K, where the entire binding process takes place inside the heme pocket. We have performed measurements of the pressure dependence of binding up to about 300 K.[62] These data again provide additional information on the rather complicated binding process, but discussion of the results is beyond the scope of this paper.

All experiments treated in the present paper share one problem (and opportunity) not yet discussed in detail. The data obtained all refer not to the properties of an isolated protein but to the protein–hydration shell–solvent system. This observation is particularly important in pressure experiments, because pressure changes the viscosity, the relaxation,[68] the pH, and the pK of the solvent.[69] The results of the present work show that the properties of Mb also depend strongly on these parameters. It will therefore be important to study the crucial features of the energy landscape, the protein dynamics, and the protein reactions with different solvents in order to understand these effects. As one example we mention that we have evaluated the binding data for Mb with the Arrhenius relation, eq 24, with the preexponential factor A_{BA} assumed to be pressure independent. Kramers' theory implies, however, that the prefactor depends on viscosity,[60] and viscosity is pressure dependent. Pressure thus affects the reaction rate not only through activation and conformation volume but also through changes in the preexponential factor,[70] and this change should also be studied. It is not unfortunate that we do not obtain information about the isolated protein because the functioning protein in a living system is not in a standard aqueous solution but is always part of a more complex system. Studies with different solvents and solvent conditions, therefore, can tell us much about possible effects of the environment on proteins within living systems.

Theoretical work is indicated in at least two different directions. In section 8, we introduced a highly simplified treatment of the effect of pressure on the reaction rate. This treatment must be extended to take the nonexponential time dependencies and the hierarchy of substates into account. A more difficult theoretical problem is the connection between the binding process and molecular dynamics computations.[71-73] Ultimately, this connection may elucidate the way in which protein structure and dynamics control protein function.

Pressure effects, to which Harry Drickamer has devoted essentially his entire scientific work, promise to be as important and fruitful in the study of proteins as they have been, and still are, in the exploration of simpler systems.

Acknowledgment. We thank Joel Berendzen, Todd Sauke, Joe Vittitow, and all other members, past and present, of the biological physics group at the University of Illinois for collaborations and discussions. We thank H. G. Drickamer, V. I. Goldanskii, D. Lazarus, C. P. Slichter, and P. G. Wolynes for illuminating discussions and comments. We gratefully acknowledge Mary Ostendorf for her efforts in manuscript preparation. R.D.Y. thanks Illinois State University for research support. S.L. thanks NSERC for a postdoctoral fellowship. Part of the paper was written at the Aspen Center for Physics (H.F.). This work was supported in part by the Office of Naval Research Grant N00014-89-R-1300, the National Science Foundation Grant DMB87-16476, and the National Institutes of Health Grants GM 18051 and 32455.

Registry No. O_2, 7782-44-7; CO, 630-08-0.

(66) Bennett, W. S.; Huber, R. *Crit. Rev. Biochem.* **1982**, *15*, 291.
(67) Alben, J. O.; Beece, D.; Bowne, S. F.; Eisenstein, L.; Frauenfelder, H.; Good, D.; Marden, M. C.; Moh, P. P.; Reinisch, L.; Reynolds, A. H.; Yue, K. T. *Phys. Rev. Lett.* **1980**, *44*, 1157.
(68) McDuffie, Jr., G. E.; Kelly, M. V. *J. Chem. Phys.* **1964**, *41*, 2666.
(69) Douzou, P. *Cryobiology*; Academic Press: New York, 1977.
(70) Karplus, M.; McCammon, J. A. *FEBS Lett.* **1981**, *131*, 34.
(71) McCammon, J. A.; Harvey, S. C. *Dynamics of Proteins and Nucleic Acids*; Cambridge: New York, 1987.
(72) Brooks, C. L.; Karplus, M.; Pettit, B. M. *Proteins: A Theoretical Perspective of Dynamics, Structure and Thermodynamics*; Wiley: New York, 1988.
(73) Catlin, B. *J. Chem. Phys.* **1989**, *91*, 427.

Distribution List for Annual and Final Reports

1. Put a cover page (Form DD 1473) on your report and attach a copy of the distribution list. Mail one copy of the report to each person on the contractor subset list attached on which your name appears. The other subset list is for your information only. Please don't forget to attach this distribution list to your report - otherwise the folks below think they have mistakenly received the copy meant for the Molecular Biology Program and forward it to us.

2. Mail two copies to (include a DTIC Form 50 with these two copies too)
   Administrator
   Defense Technical Information Center
   Building 5, Cameron Station
   Alexandria, VA 22314

3. Mail one copy to each of the following:

(a) Dr. Michael Marron
ONR Code 1141
Molecular Biology Program
800 N. Quincy Street
Arlington, VA 22217-5000

(b) Administrative Contracting Officer
ONR Resident Representative
(address varies - see copy of your grant)

(c) Director,
Applied Research Directorate
ONR Code 12
800 N. Quincy Street
Arlington, VA 22217-5000

(d) Director
Office of Naval Technology
Code 22
800 N. Quincy Street
Arlington, VA 22217-5000

(e) Director
Chemical and Biological Sci Div
Army Research Office
P. 0. Box 12211
Research Triangle Park, NC 27709

(f) Life Sciences Directorate
Air Force Office of Scientific Research
Bolling Air Force Base
Washington, DC 20332

(g) Director
Naval Research Laboratory
Technical Information Div, Code 2627
Washington, DC 20375

AMZEL, L. Mario
Department of Biophysics
Johns Hopkins School of Medicine
725 North Wolfe Street
Baltimore, MD 21205

ANDERSEN, Niels H.
Department of Chemistry
University of Washington
Seattle, WA 98195

ARNOLD, Frances H.
Dept of Chemical Engineering
California Institute of Technology
Pasadena, CA 91125

AUGUST, J. Thomas
Department of Pharmacology
Johns Hopkins Medical School
725 North Wolfe Street
Baltimore, MD 21205

BEVERIDGE, David L
Department of Chemistry
Wesleyan University
Hall-Altwater Laboratories
Middletown, CT 06457

BRAMSON, H. Neal
Department of Biochemistry
Univ of Rochester Medical Center
601 Elmwood Avenue
Rochester, NY 14642

BRUICE, Thomas C.
Department of Chemistry
University of California-Santa Barbara
Santa Barbara, CA 93106

CASE, Steven T.
Department of Biochemistry
Univ of Mississippi Medical Center
2500 North State Street
Jackson, MS 39216-4505

CHANG, Eddie L.
Bio/Molecular Engineering
Naval Research Laboratory
Code 6190
Washington, D.C. 20375-5000

CHRISTIANSON, David W.
Department of Chemistry
University of Pennsylvania
231 South 34th Street
Philadelphia, PA 19104-6323

CORDINGLEY, John S.
Department of Molecular Biology
University of Wyoming
Box 3944 University Station
Laramie, WY 82071

DeGRADO, William F.
E. I. du Pont de Nemours & Co
Central R & D, Experimental Station
P. O. Box 80328
Wilmington, DE 19880-0328

EVANS, David R.
Department of Biochemistry
Wayne State Univ School of Medicine
540 E. Canfield Street
Detroit, Michigan 48201

FEIGON, Juli F.
Department of Chem & Biochemistry
UCLA
405 Hilgard Avenue
Los Angeles, CA 900024-1569

FICHT, Allison R.
Dept of Med Biochem & Genetics
Texas A&M University
College Station, TX 77843

FRAUENFELDER, Hans
Department of Physics
University of Illinois
Urbana, IL 61801

GABER, Bruce
Naval Research Laboratory
Bio/Molecular Engineering Branch
Code 6190
Washington, DC 20375

GETZOFF, Elizabeth D.
Scripps Clinic & Research Foundation
Department of Molecular Biology
10666 North Torrey Pines Road
La Jolla, CA 92037

GOODMAN, Eugene M.
Biomedical Research Institute
University of Wisconsin
P. O. Box 2000
Kenosha, WI 53141

HO, Pui Shing
Department of Biochemistry and Biophysics
Oregon State University
Corvallis, OR 97331

HOGAN, Michael E.
Baylor Center for Biotechnology
4000 Research Forest Drive
The Woodlands, TX 77381

HONIG, Barry
Columbia University
Dept of Biochem and Molec Biophys
630 West 168th St.
New York, NY 10032

HOPKINS, Paul B.
Department of Chemistry
University of Washington
Seattle, WA 98195

KAHNE, Daniel
Department of Chemistry
Princeton University
Princeton, NJ 08544

KEMP, Robert G.
Chicago Medical School
Dept of Biological Chemistry
3333 Green Bay Rd.
North Chicago, IL 60064

KHORANA, Gobind H.
Department of Biology
MIT
77 Massachusetts Ave.
Cambridge, MA 02139

KIM, Sangtae
Chemical Engineering
University of Wisconsin
1415 Johnson Drive
Madison, WI 53706

LANSBURY, Peter T.
Department of Chemistry
MIT
Cambridge, MA 02139

LAURSEN, Richard A.
Chemistry Department
Boston University
590 Commonwealth Avenue
Boston, MA 02215

LENZ, Robert W.
Chemical Engineering Department
University of Massachusetts
Amherst, MA 01003

LEWIS, Randolf V.
Molecular Biology Department
University of Wyoming
University Station Box 3944
Laramie, WY 82071

LINDSAY, Stuart M.
Department of Physics
Arizona State University
Temp, AZ 85278

LOEB, George I.
David W. Taylor Research Center
Code 2841
Annapolis, MD 21402-5067

MASILAMANI, Divakar
Biotechnology Department
Allied-Signal Inc.
P. O. Box 1021R
Morristown, NJ 07960

McCONNELL, Harden M.
Stanford University
Department of Chemistry
Stanford, CA 94305

McELROY, Willam D.
Department of Chemistry
University of California - San Diego
La Jolla, CA 92093-0601

MERTES, Kristin Bowman
University of Kansas
Dept of Chemistry
Lawrence, Kansas 66045

NAGUMO, Mark
Bio/Molecular Engineering Branch
Naval Research Laboratory
Code 6190
Washington, DC 20375-5000

OLIVERA, Baldomero M.
Department of Biology
University of Utah
Salt Lake City, UT 84112

PABO, Carl O.
Department of Biophysics
Johns Hopkins University
School of Medicine
Baltimore, MD 21205

PRENDERGAST, Franklyn G.
Dept of Biochemistry & Molec Biol
Mayo Foundation
200 First St. SW
Rochester, MN 55905

PUGH, Jr., Edward N.
Deaprtment of Psychology
University of Pennsylvania
3815 Walnut Street
Philadelphia, PA 19104-6196

RACKOVSKY, Shalom R.
Department of Biophysics
University of Rochester
School of Medicine and Dentistry
Rochester, NY 14642

RAJAN, K. S.
Illinois Institute of Technology
Research Institute
10 W. 35th St.
Chicago, IL 60616

REINISCH, Lou
Laser Biophysics Center
Uniformed Services University
4301 Jones Bridge Road
Bethesda, MD 20814

RICH, Alexander
MIT Department of Biology
Cambridge, MA 02139

RICHARDS, J. H.
California Institute of Technology
Division of Chemistry and Chemical Engineering
Pasadena, CA 91125

ROTHSCHILD, Kenneth J.
Department of Physics
Boston University
590 Commonwealth Avenue
Boston, MA 02215

SCHULTZ, Peter G.
Department of Chemistry
University of California-Berkeley
Bekeley, CA 94720

SEEMAN, Nadrian
Department of Chemistry
New York University
New York, NY 10003

SELSTED, Michael E.
UCLA
Dept of Medicine
37-055 CHS
Los Angeles, CA 90024

SIGMAN, David S.
UCLA School of Medicine
Dept of Biological Chemistry
Los Angeles, CA 90024
SIKES, Steven C.
Department of Biological Sciences
University of South Alabama
Mobile, AL 36688

SINSKEY, Anthony J.
Laboratory of Applied Microbiology
MIT Department of Biology
Cambridge, MA 02139

STEWART, James M.
Department of Chemistry
University of Maryland
College Park, MD 20742

STEWART, John M.
Department of Biochemistry
University of Colorado
Health Science Center
Denver, CO 80262

TURNER, Douglas H.
Department of Chemistry
University of Rochester
Rochester, NY 14627

URRY, Dan W.
Laboratory of Molecular Biophysics
University of Alabama
P. O. Box 311
Birmingham, AL 35294

WAITE, J. Herbert
College of Marine Studies
University of Deleware
Lewes, DE 19958

WARD, Keith B.
Naval Research Laboratory
Code 6030
Washington, DC 20375

WARSHEL, Arieh
Department of Chemistry
University of Southern California
University Park
Los Angeles, CA 90089-0482

WATT, Gerald D.
Dept of Chemistry & Biochemistry
University of Colorado
Campus Box 215
Boulder, CO 80309-0215